Novel Techniques for Snow Cover Mapping Using Polarimetric SAR Images

Prof. Avik Bhattacharya
Microwave Remote Sensing Lab
Centre of Studies in Resources Eng.
Indian Institute of Technology Bombay
Mumbai-400076, India
www.mrslab.in

MRSLab

IIT Bombay

LISTIC, Université Savoie Mont Blanc, Annecy, France
11th June 2019

The Elements of Cryosphere: Snow Fields & Glaciers

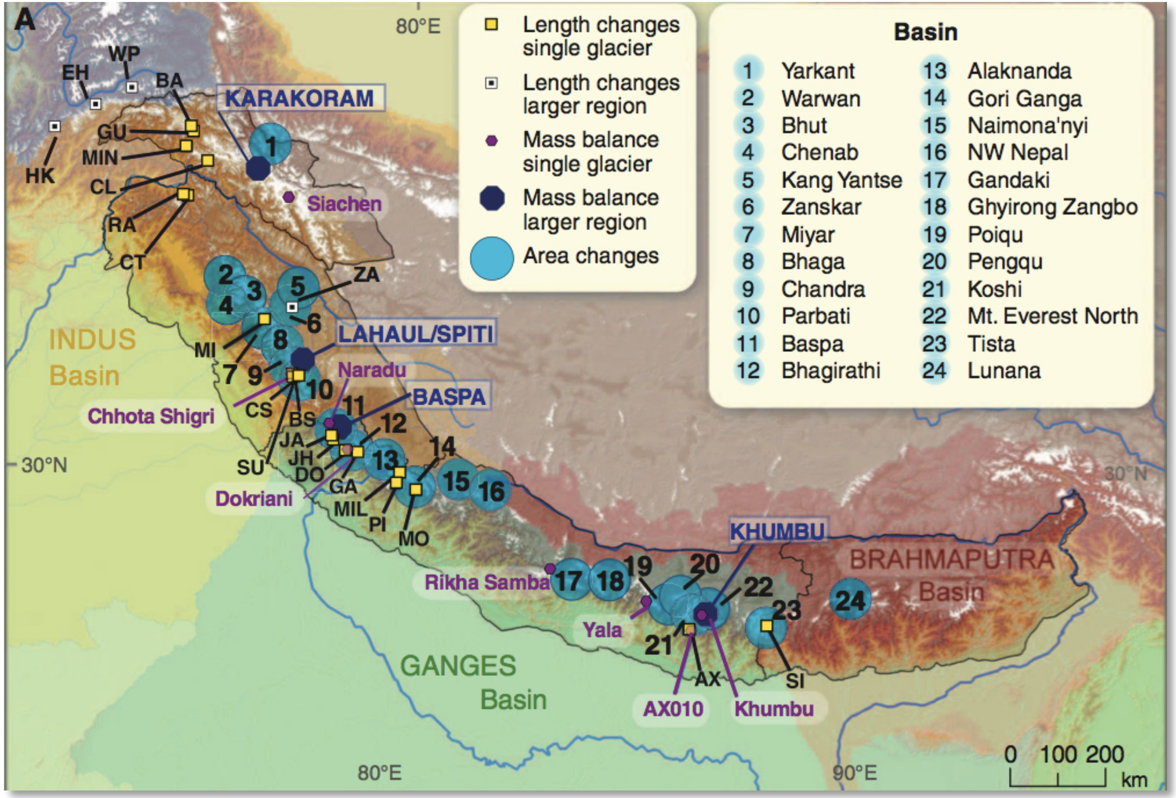

Hindu-Kush Himalayas: The 3rd Pole

Test Site

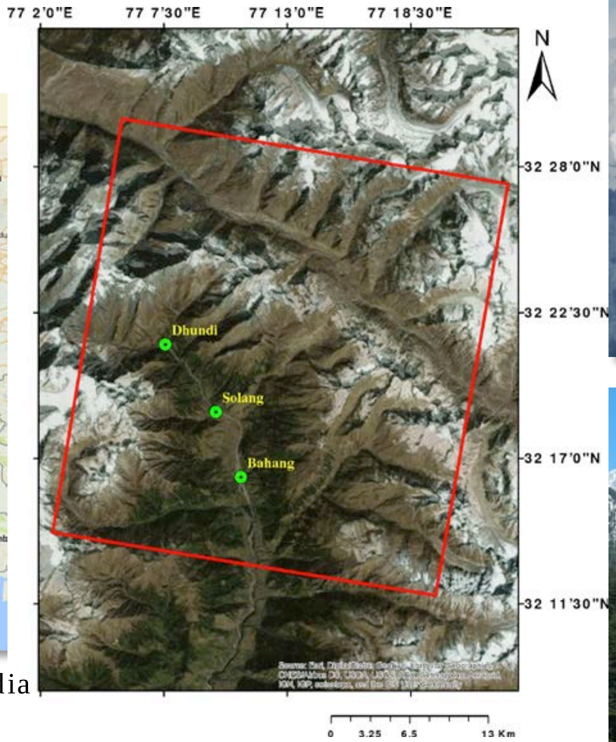

Area: Manali-Dhundi region, Himachal Pradesh, India
Elevation: 2000 to 5000 m
Land-cover: Approx. 30% is coniferous vegetation with bare ground above the mean tree line
Vegetation Characteristics: Needle-like leaves & clamped structure with average height of 50-60 m. Remains snow-free during winters
Observatories: Bahang (2000 m), Solang (2450 m), and Dhundi (2900 m) maintained by SASE, DRDO, India

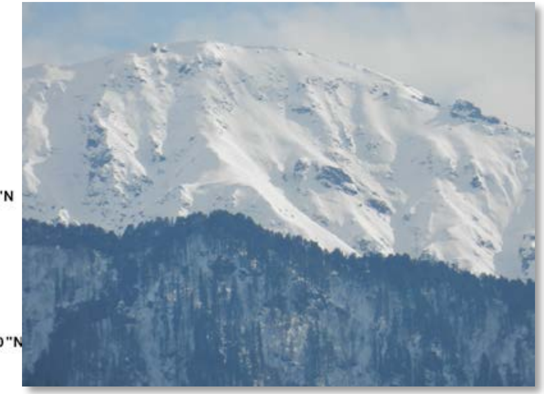

Tall coniferous trees (~30-50 m tall) spread across the **Beas river valley** below the mean tree line

IIT Bombay

PolSAR Data Representation: Coherency/Covariance/Kennaugh matrix

$$[\mathbf{S}] = \begin{bmatrix} S_{XX} & S_{XY} \\ S_{YX} & S_{YY} \end{bmatrix} \Longrightarrow \boldsymbol{k}_P = V([\mathbf{S}]) = \frac{1}{2}\mathrm{Tr}([\mathbf{S}]\Psi_P) \Rightarrow \langle[\mathbf{T}]\rangle = \frac{1}{N}\sum_{i=1}^{N} \boldsymbol{k}_{Pi} \cdot \boldsymbol{k}_{Pi}^{*T}$$

$$[\mathbf{S}] = \begin{bmatrix} S_{XX} & S_{XY} \\ S_{YX} & S_{YY} \end{bmatrix} \Longrightarrow \boldsymbol{k}_L = V([\mathbf{S}]) = \frac{1}{2}\mathrm{Tr}([\mathbf{S}]\Psi_L) \Rightarrow \langle[\mathbf{C}]\rangle = \frac{1}{N}\sum_{i=1}^{N} \boldsymbol{k}_{Li} \cdot \boldsymbol{k}_{Li}^{*T}$$

$$\Downarrow$$

$$\langle[\mathbf{K}]\rangle = \begin{bmatrix} k_{11} & k_{12} & k_{13} & k_{14} \\ k_{12} & k_{22} & k_{23} & k_{24} \\ k_{13} & k_{23} & k_{33} & k_{34} \\ k_{14} & k_{24} & k_{34} & k_{44} \end{bmatrix} \in \mathbb{R}^{10}$$

PolSAR Data Representation: Coherency/Covariance/Kennaugh matrix

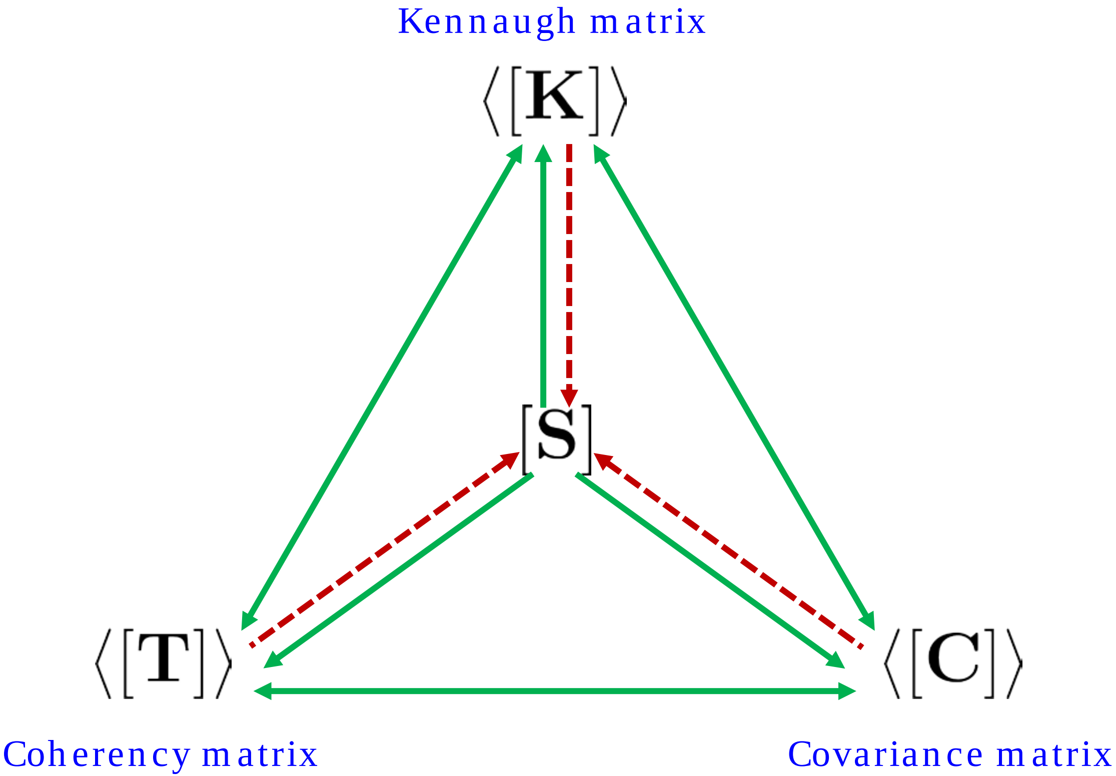

Geometry of PolSAR Data

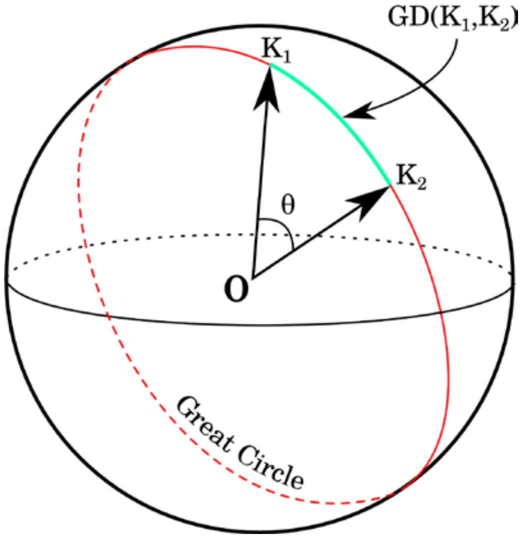

$$GD(\mathbf{K_1}, \mathbf{K_2}) = \frac{2}{\pi} \cos^{-1}\left(\frac{Tr(\mathbf{K_1}^T\mathbf{K_2})}{\sqrt{Tr(\mathbf{K_1}^T\mathbf{K_1})}\sqrt{Tr(\mathbf{K_2}^T\mathbf{K_2})}}\right) \in [0, 1]$$

$$\left\{\begin{array}{l} \text{Scale invariant: } GD(\lambda_1\mathbf{K}_1, \lambda_2\mathbf{K}_2) = GD(\mathbf{K}_1, \mathbf{K}_2) \\ GD(\lambda\mathbf{K}_1, \mathbf{K}_1) = 0 \text{ where } \lambda \in \mathbb{R} \end{array}\right.$$

$$\text{Unit sphere : } S^{15} = \left\{(x_1, x_2, \ldots, x_{16}) \in \mathbb{R}^{16} \mid \sqrt{x_1^2 + x_2^2 + \cdots + x_{16}^2} = 1\right\}$$

Unsupervised Classification of PolSAR Data Using a Scattering Similarity Measure Derived from a Geodesic Distance,
D. Ratha, A. Bhattacharya and A. C. Frery, *IEEE Geoscience and Remote Sensing Letters*, vol. 15, no. 1, pp. 151-155, 2018

Change Detection in Polarimetric SAR Images Using a Geodesic Distance Between Scattering Mechanisms,
D. Ratha, S. De, T. Celik and A. Bhattacharya, *IEEE Geoscience and Remote Sensing Letters*, vol. 14, no. 7, pp. 1066-1070, 2017

1

Snow Cover Change Analysis

IIT Bombay

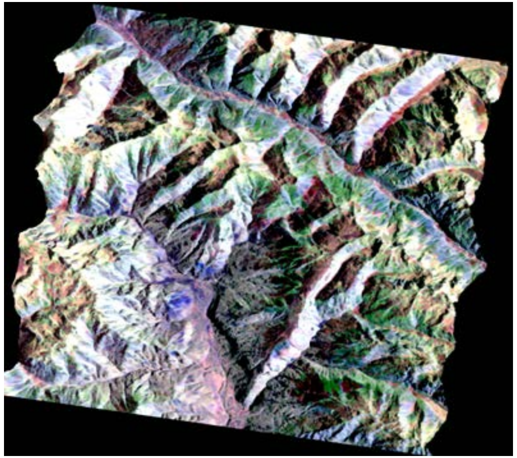

Feb-Aug

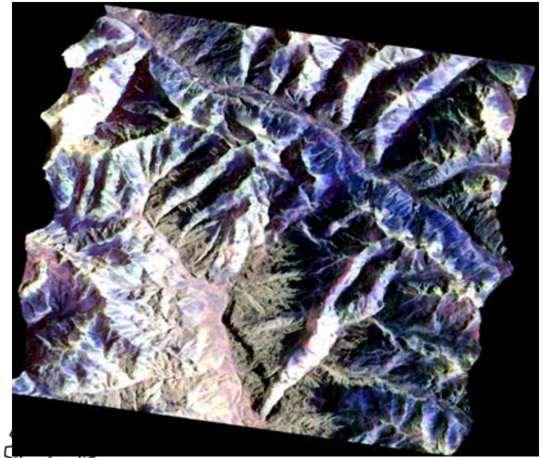

$GD(K_{Feb}, K_{Aug})_{FP}$

$GD(K_{Feb}, K_{Aug})_{HH-VV}$

Snow Cover Map

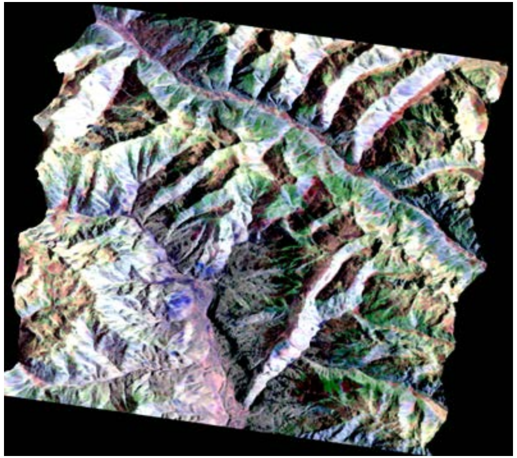

Feb-Aug

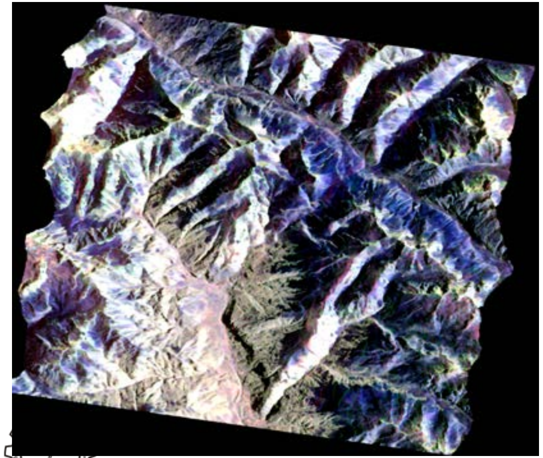

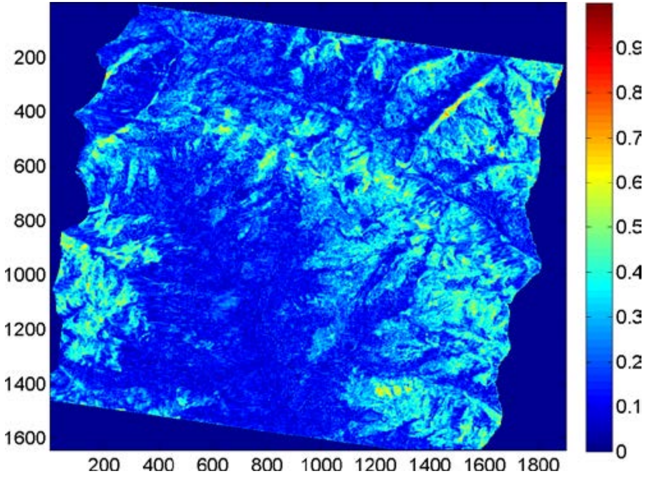

$GD(K_{Feb}, K_{Aug})_{FP}$

$GD(K_{Feb}, K_{Aug})_{HH-VV}$

Snow Cover Map

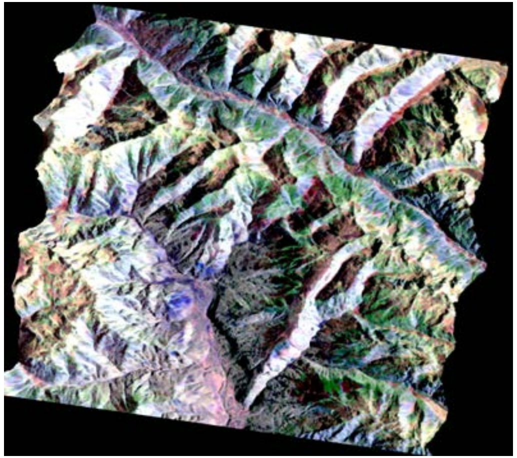

Feb-Aug

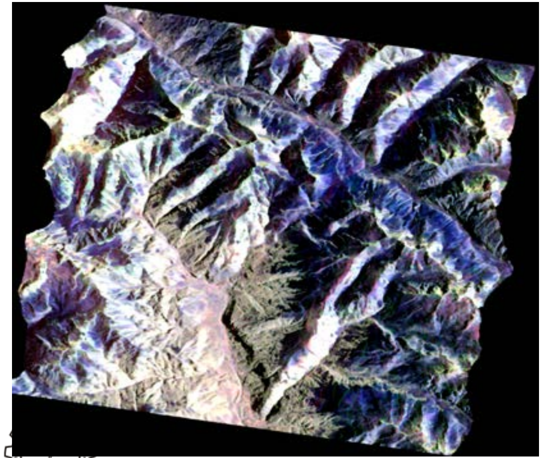

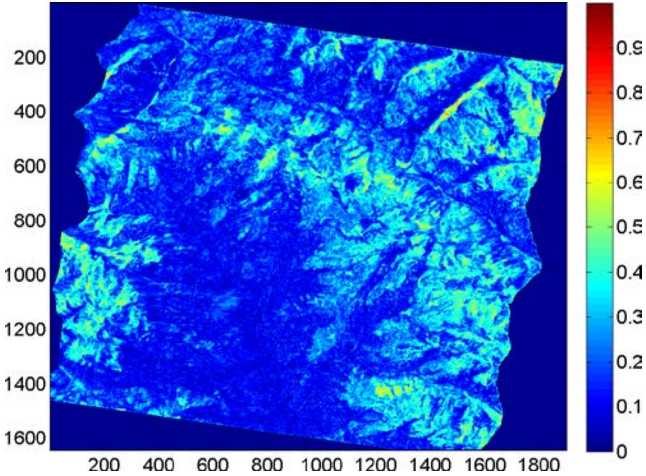

$GD(K_{Feb}, K_{Aug})_{FP}$

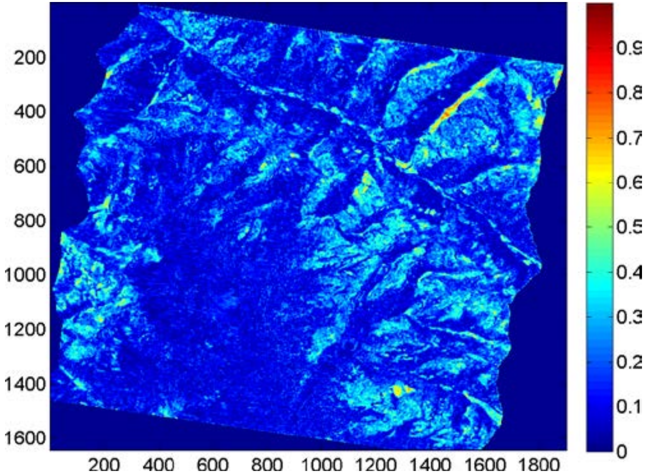

$GD(K_{Feb}, K_{Aug})_{HH-VV}$

Snow Cover Map

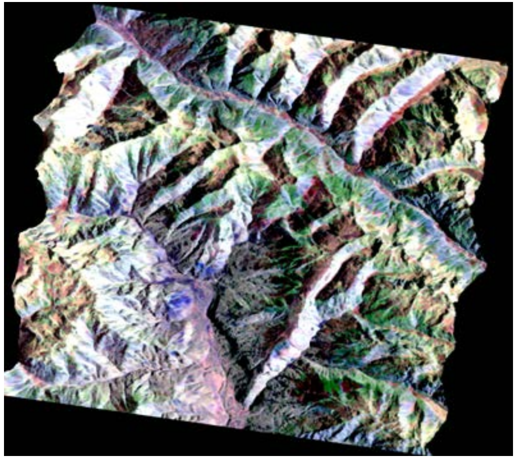

Feb-Aug

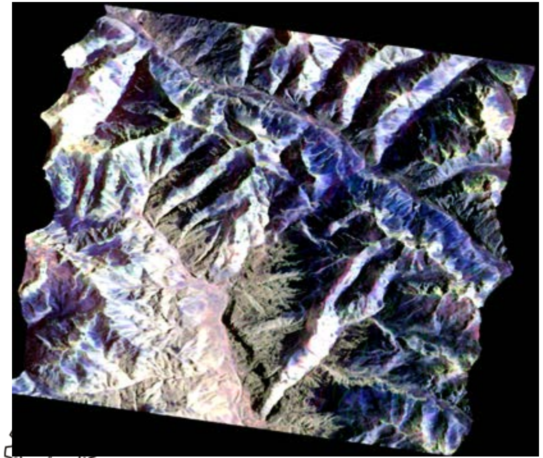

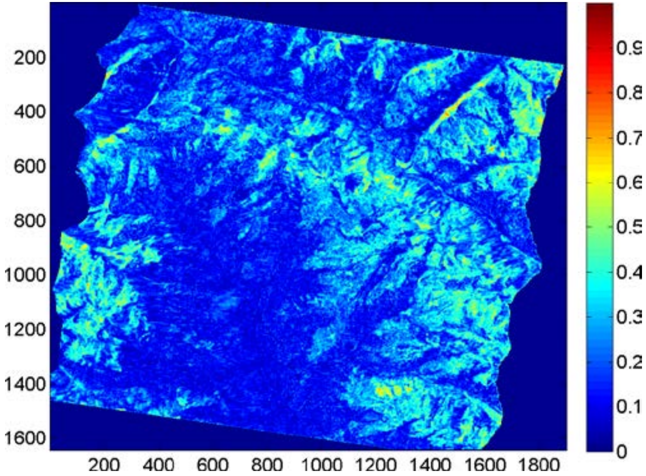

$GD(K_{Feb}, K_{Aug})_{FP}$

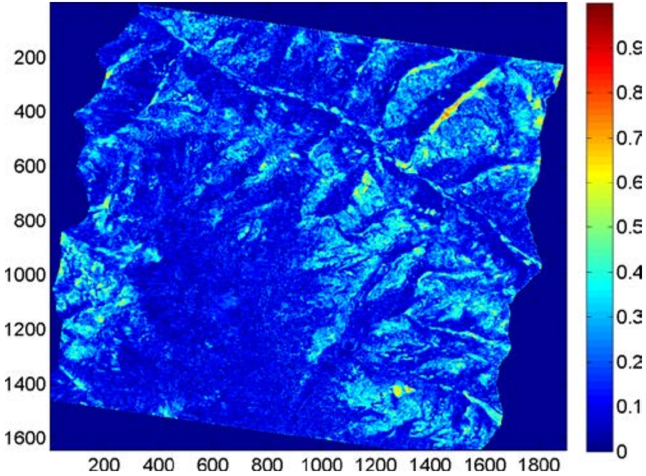

$GD(K_{Feb}, K_{Aug})_{HH-VV}$

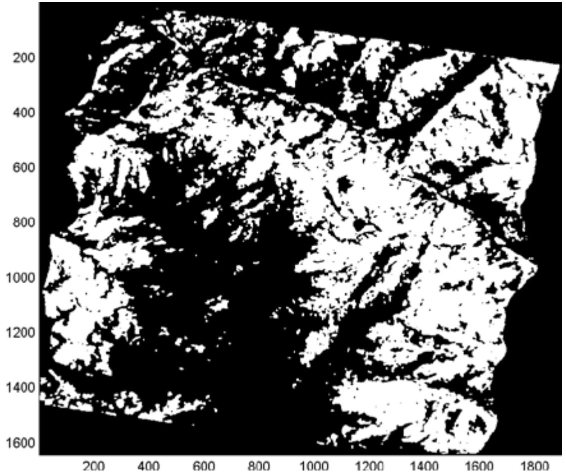

Snow Cover Map

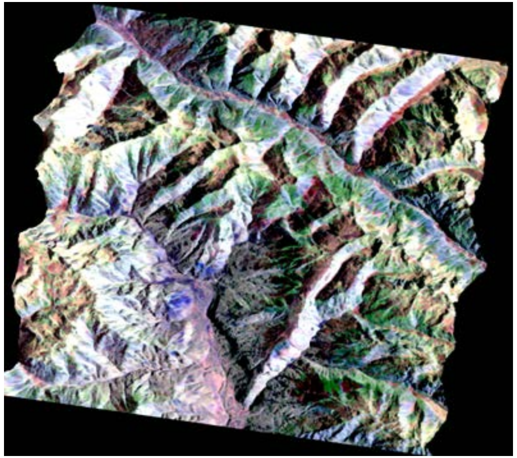

Feb-Aug

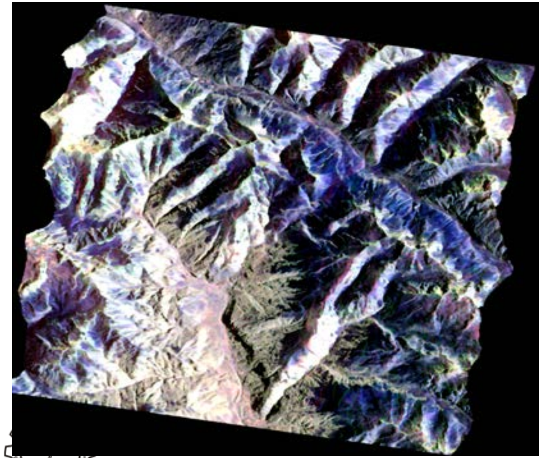

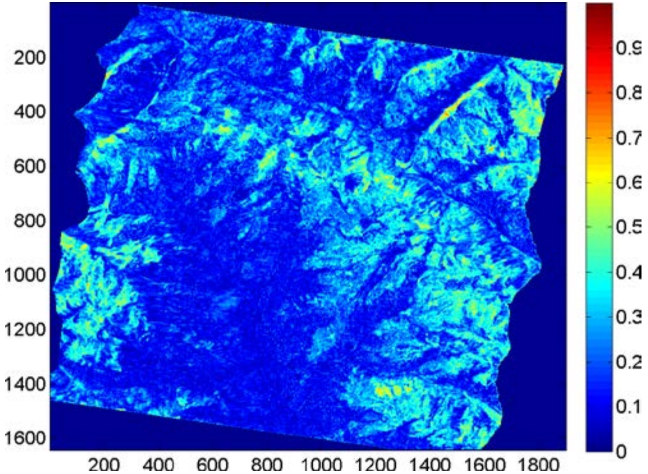

$GD(K_{Feb}, K_{Aug})_{FP}$

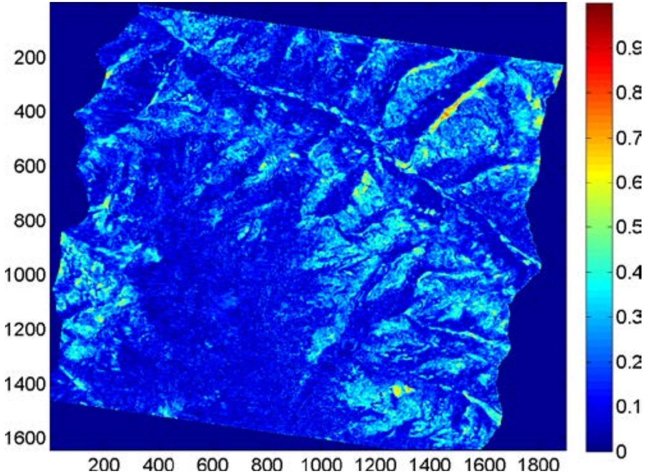

$GD(K_{Feb}, K_{Aug})_{HH-VV}$

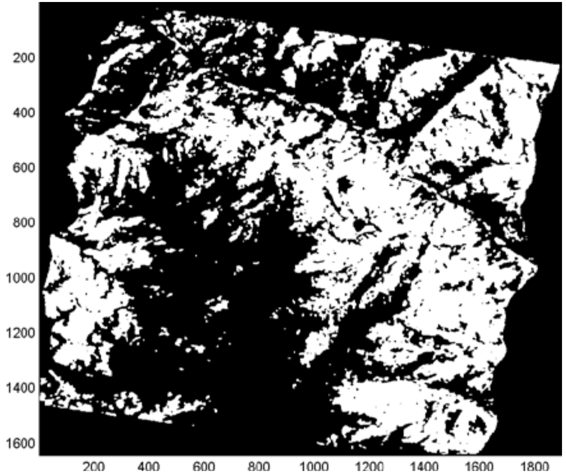

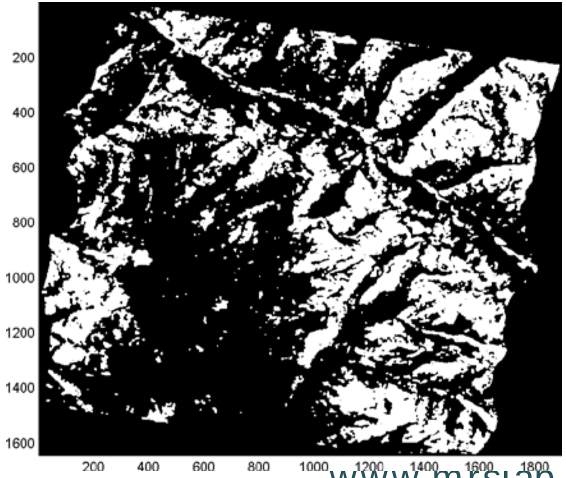

Snow Cover Map

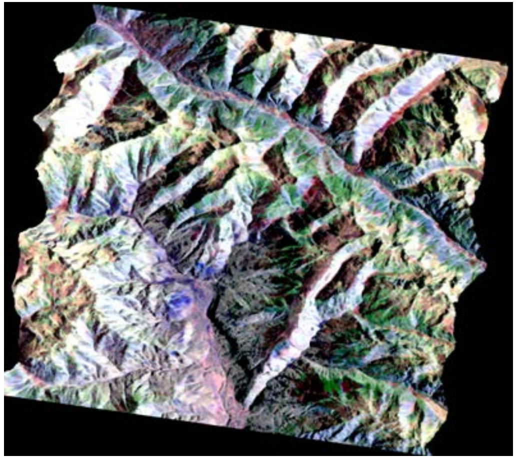

Feb-Aug

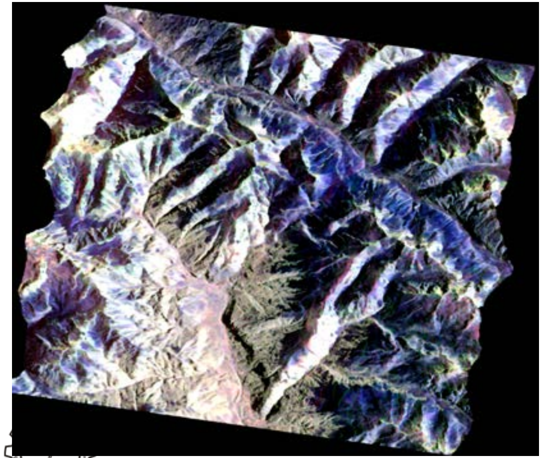

Snow Cover Map

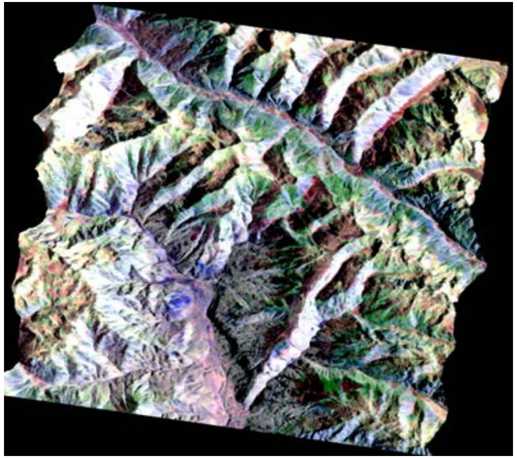

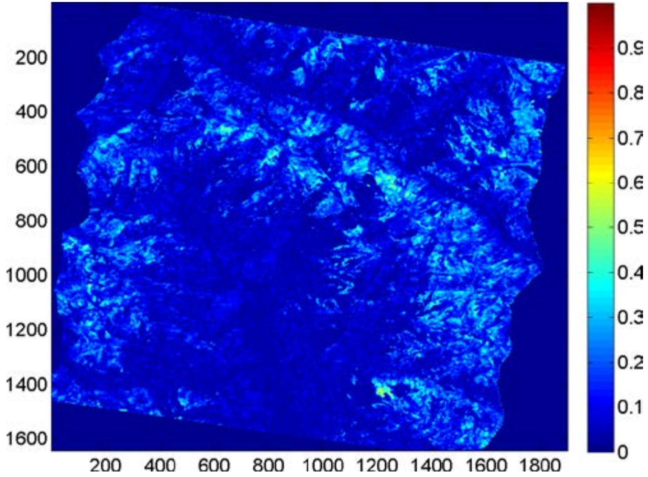

$GD(K_{Feb}, K_{Aug})_{HH-HV}$

$GD(K_{Feb}, K_{Aug})_{VV-HV}$

Feb-Aug

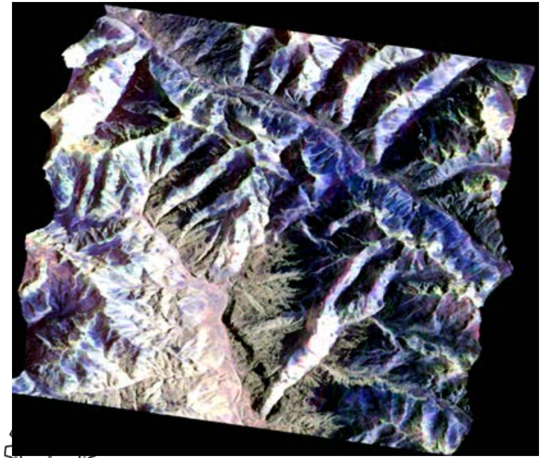

Snow Cover Map

IIT Bombay

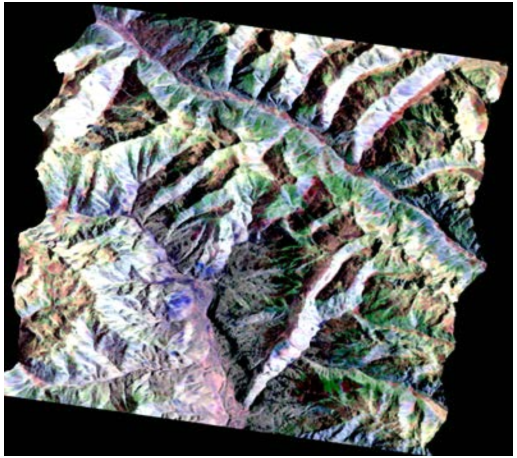

Feb-Aug

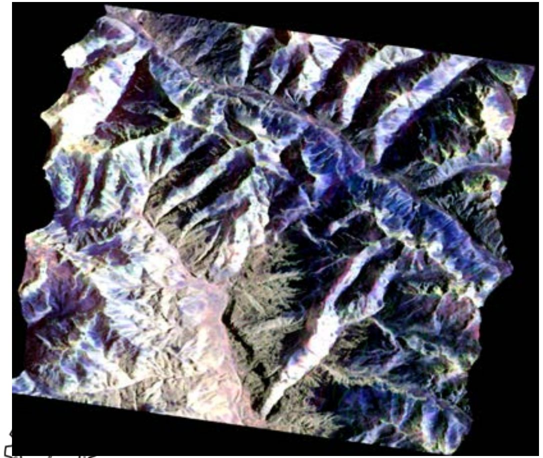

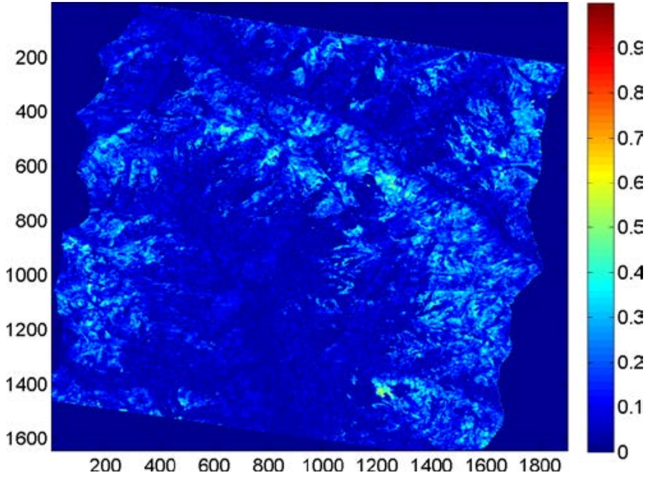

$GD(K_{Feb}, K_{Aug})_{HH-HV}$

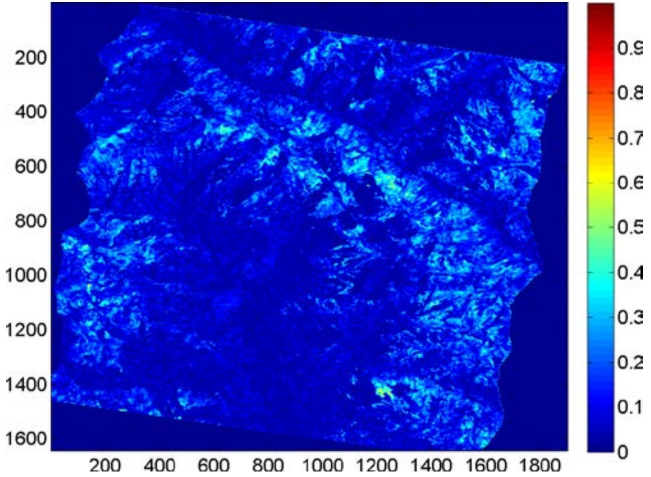

$GD(K_{Feb}, K_{Aug})_{VV-HV}$

Snow Cover Map

IIT Bombay

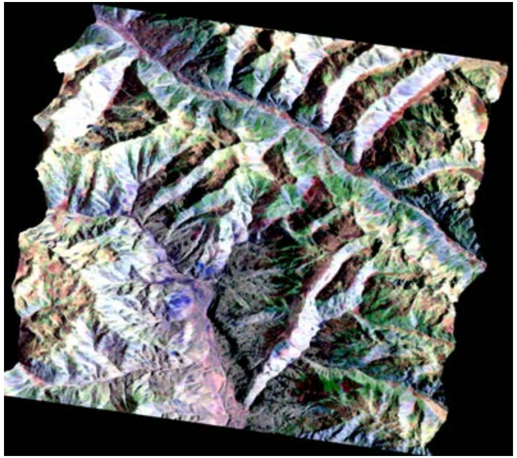

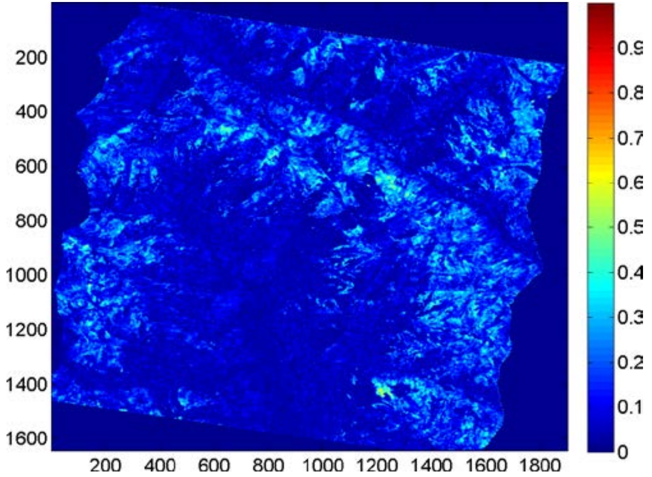

$GD(K_{Feb}, K_{Aug})_{HH-HV}$

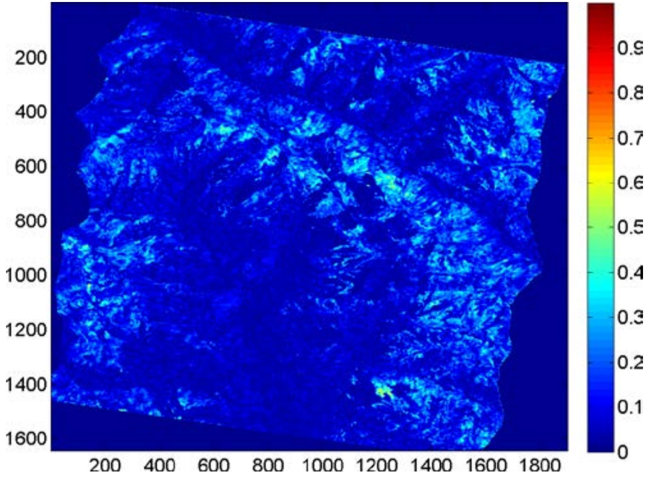

$GD(K_{Feb}, K_{Aug})_{VV-HV}$

Feb-Aug

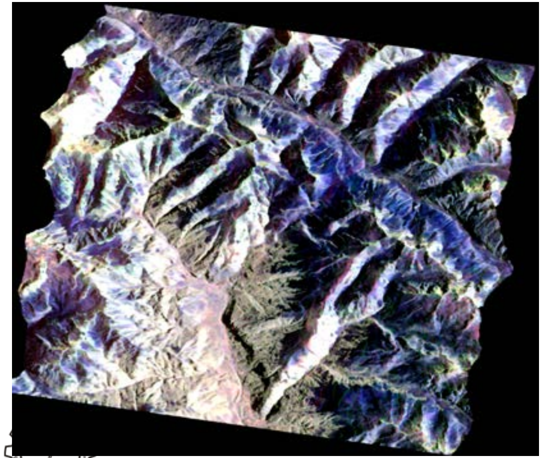

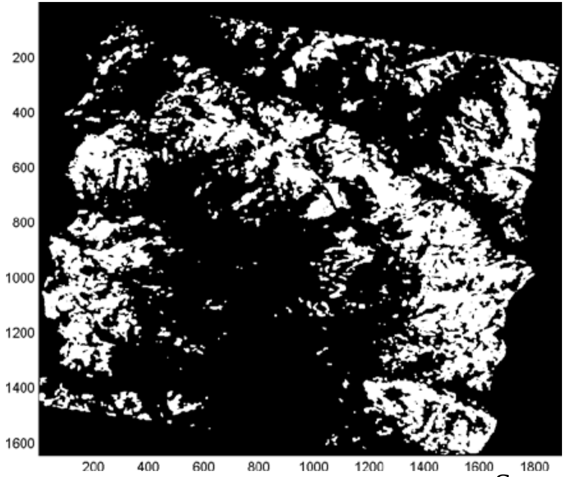

Snow Cover Map

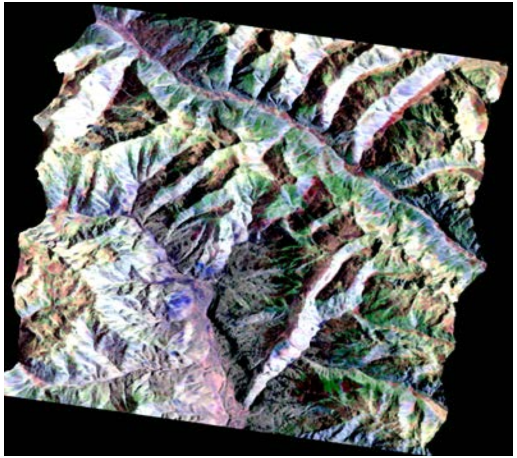

Feb-Aug

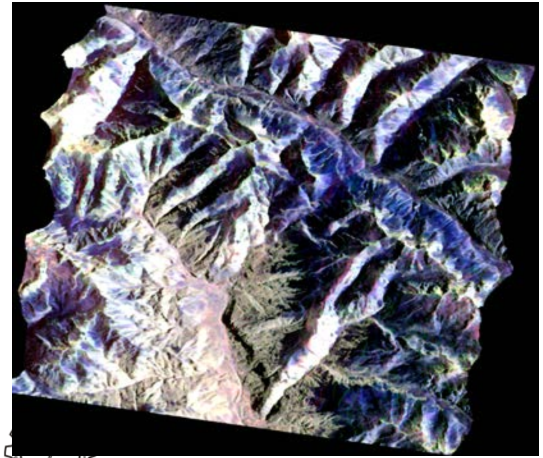

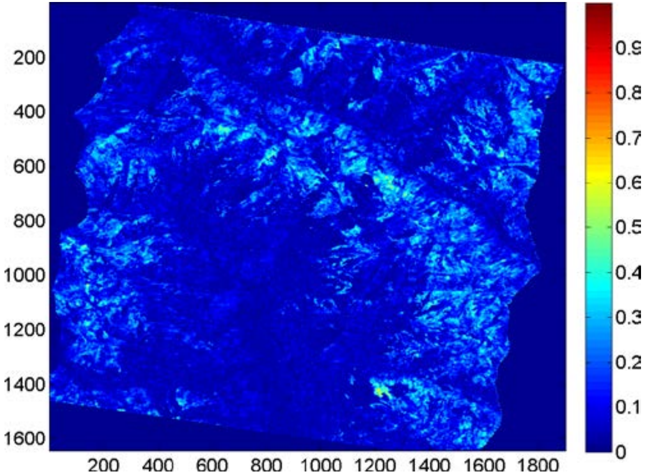

$GD(K_{Feb}, K_{Aug})_{HH-HV}$

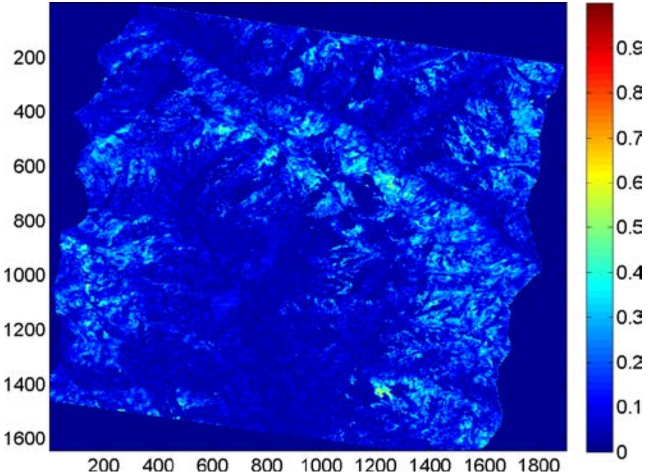

$GD(K_{Feb}, K_{Aug})_{VV-HV}$

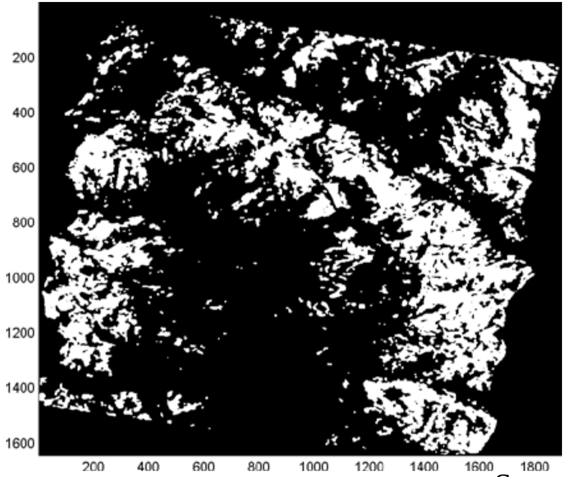

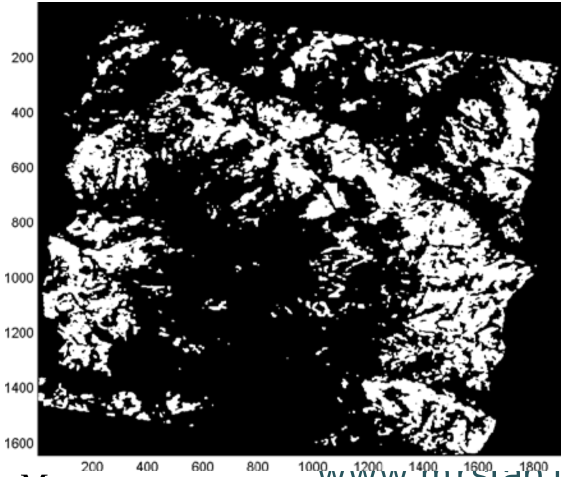

Snow Cover Map

FP

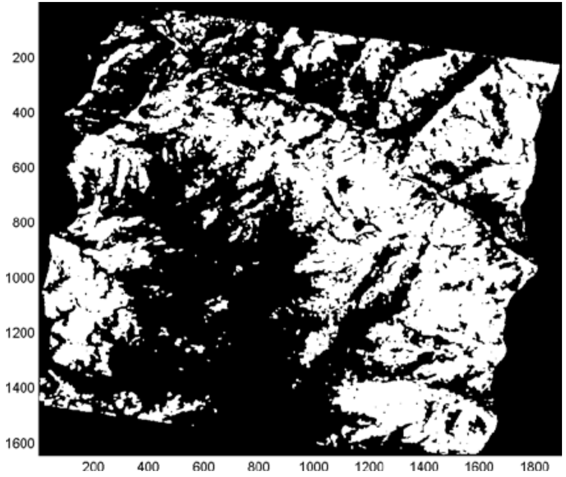

HH-VV

HH-HV

VV-VH

Snow Cover Map

FP

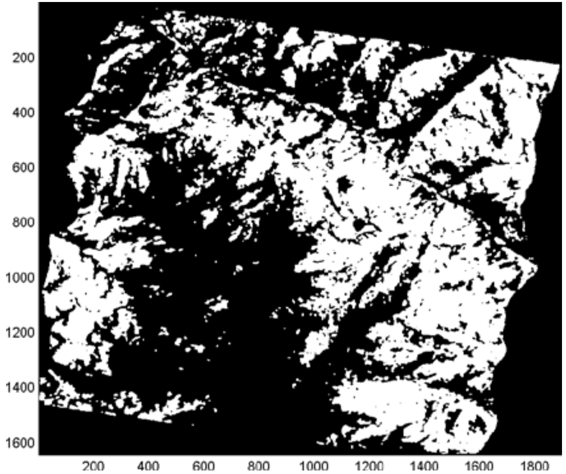

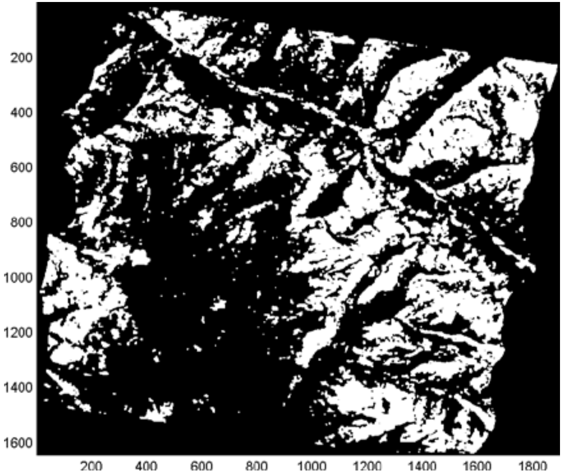

HH-VV

HH-HV

VV-VH

Snow Cover Map

FP

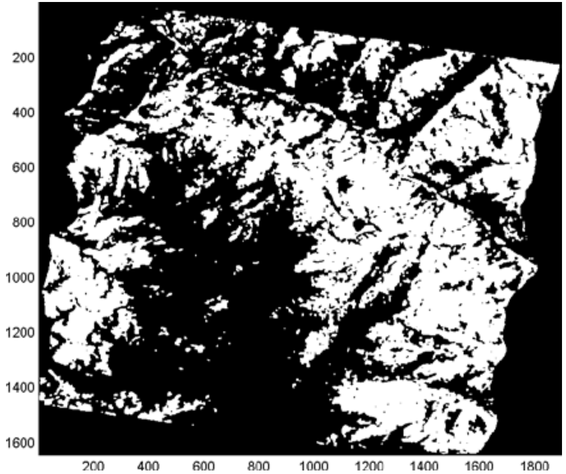

HH-VV

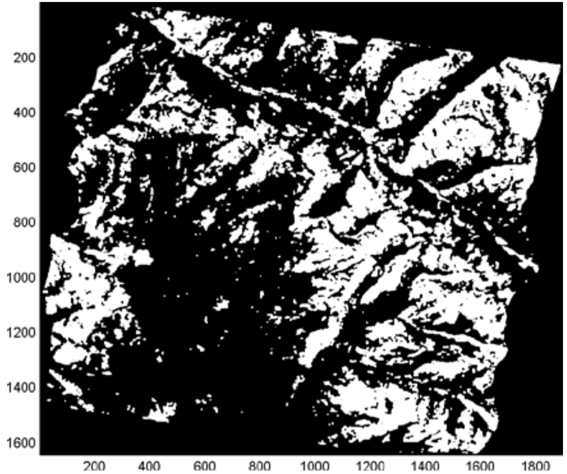

HH-HV

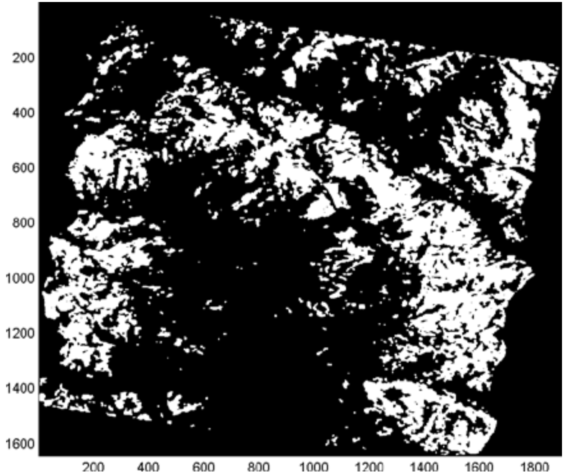

VV-VH

Snow Cover Map

FP

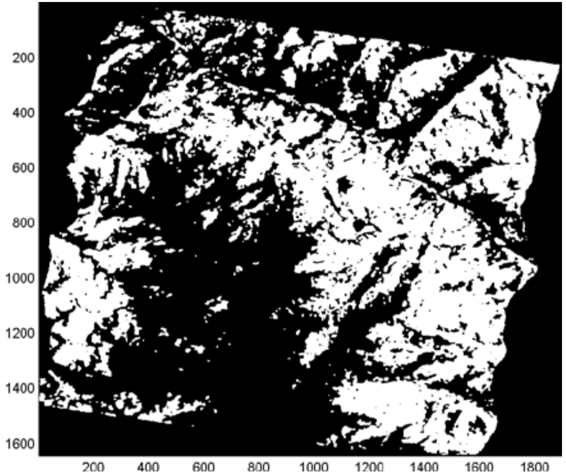

HH-VV

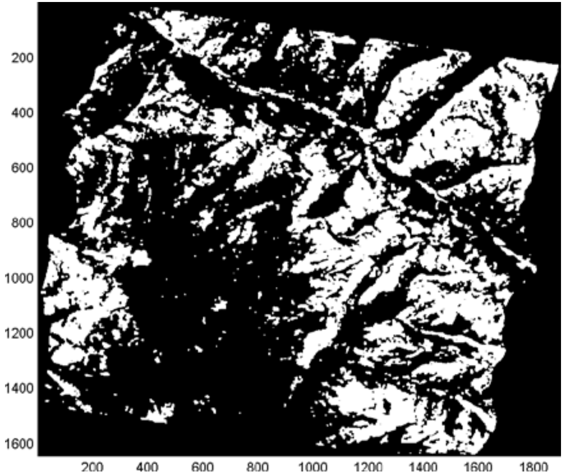

HH-HV

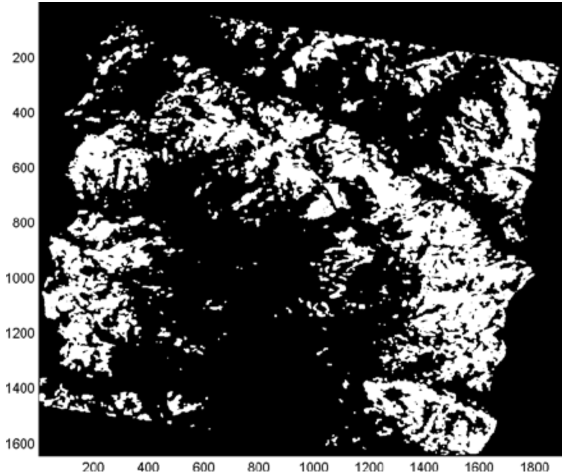

VV-VH

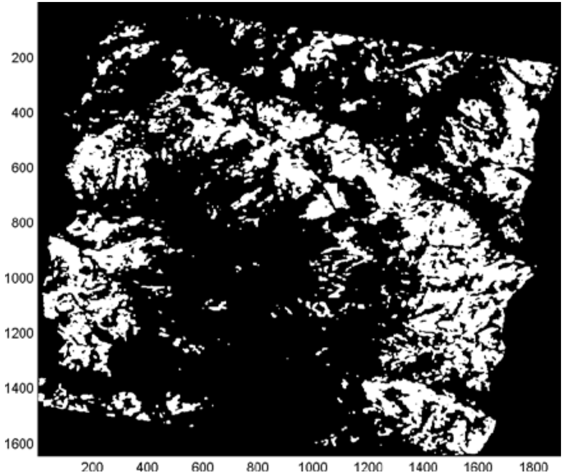

Snow Cover Map

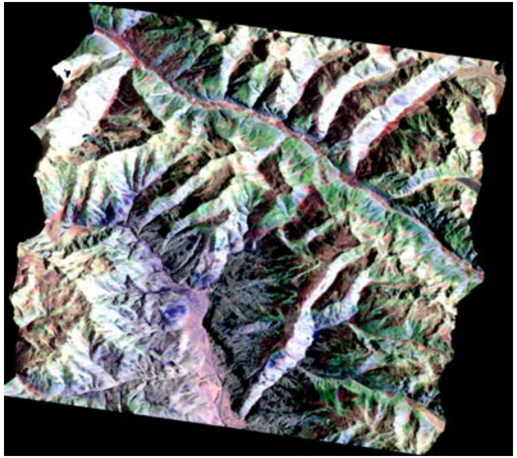

Mar-Aug

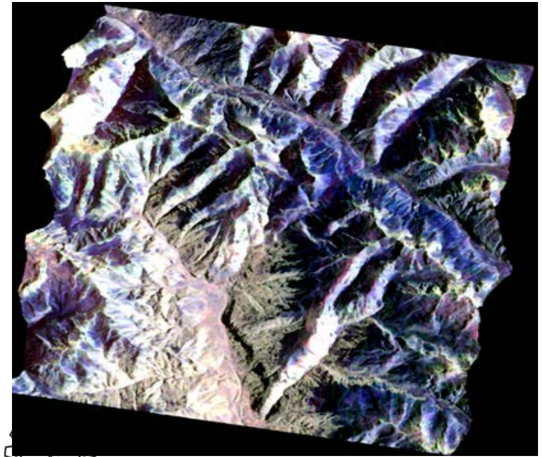

$GD(K_{Mar}, K_{Aug})_{FP}$

$GD(K_{Mar}, K_{Aug})_{HH-VV}$

Snow Cover Map

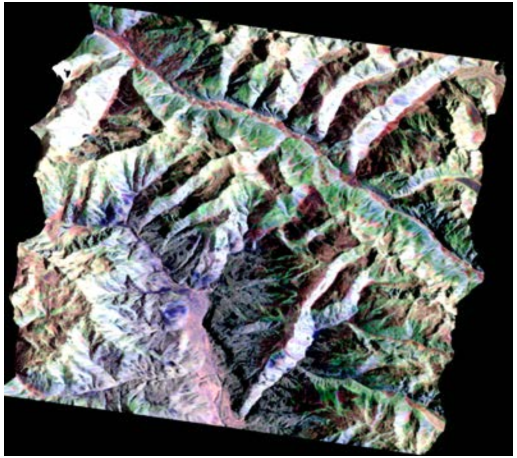

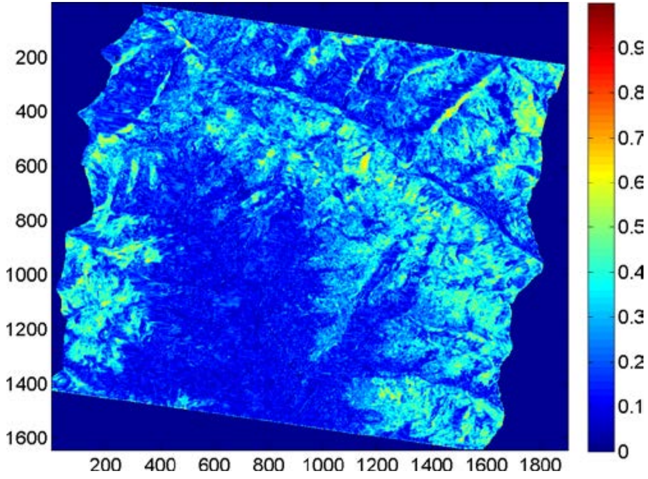

$GD(K_{Mar}, K_{Aug})_{FP}$

$GD(K_{Mar}, K_{Aug})_{HH-VV}$

Mar-Aug

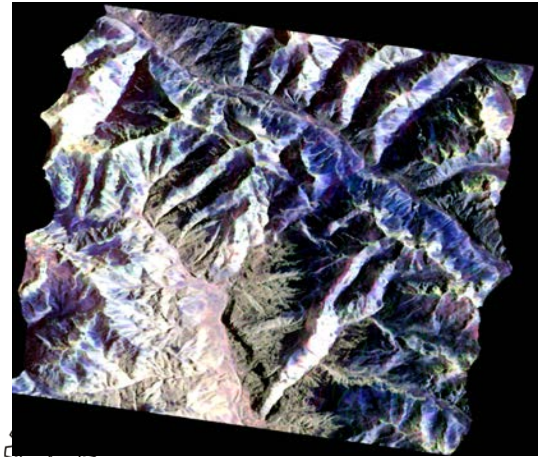

Snow Cover Map

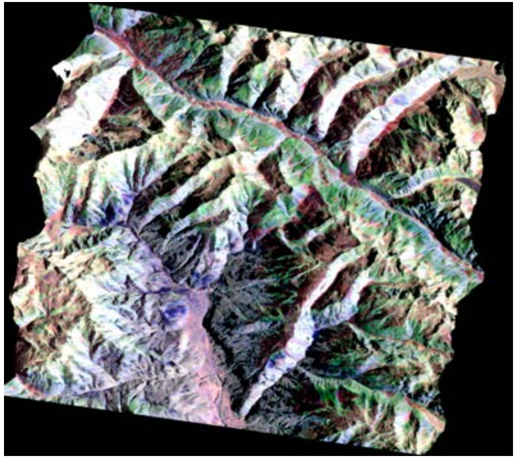

Mar-Aug

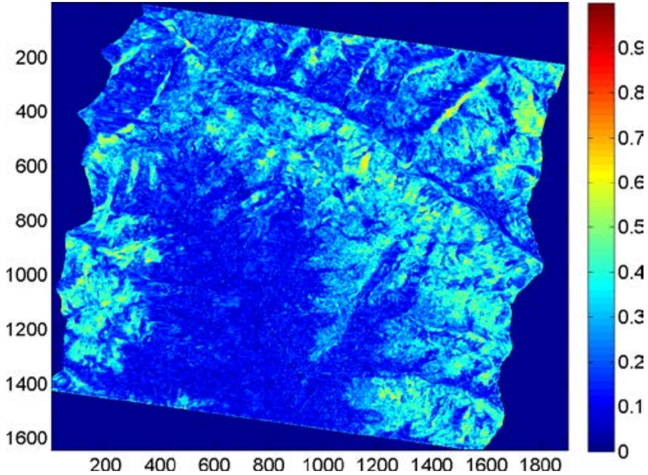

$GD(K_{Mar}, K_{Aug})_{FP}$

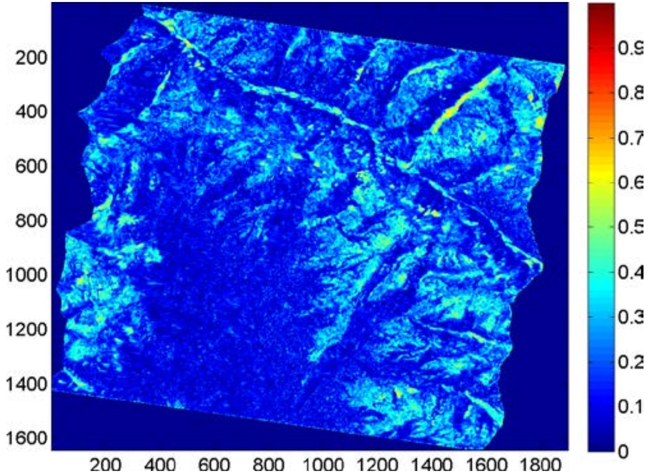

$GD(K_{Mar}, K_{Aug})_{HH-VV}$

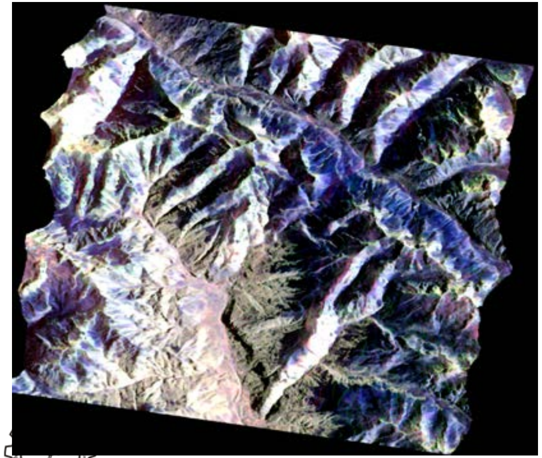

Snow Cover Map

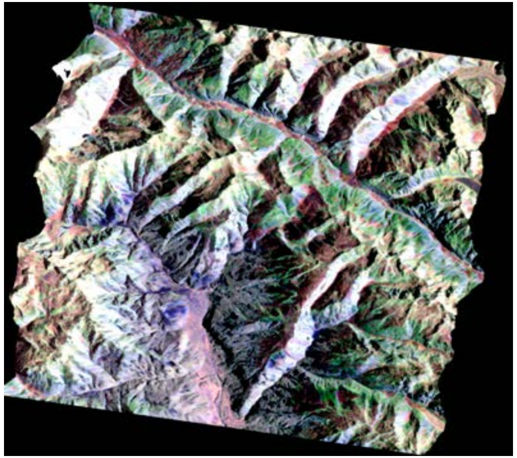

Mar-Aug

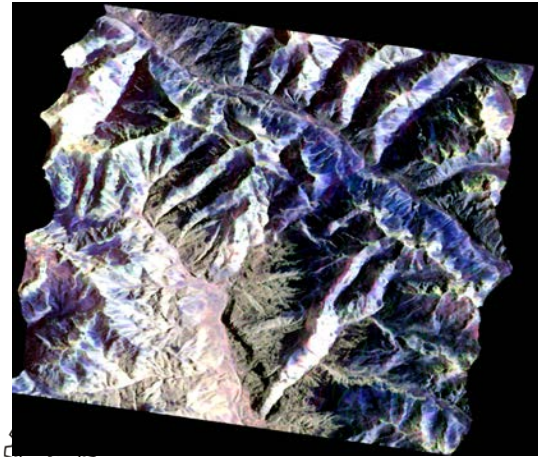

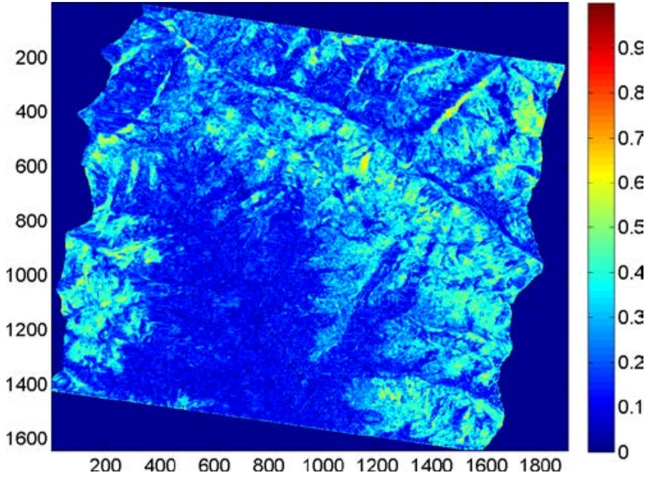

$GD(K_{Mar}, K_{Aug})_{FP}$

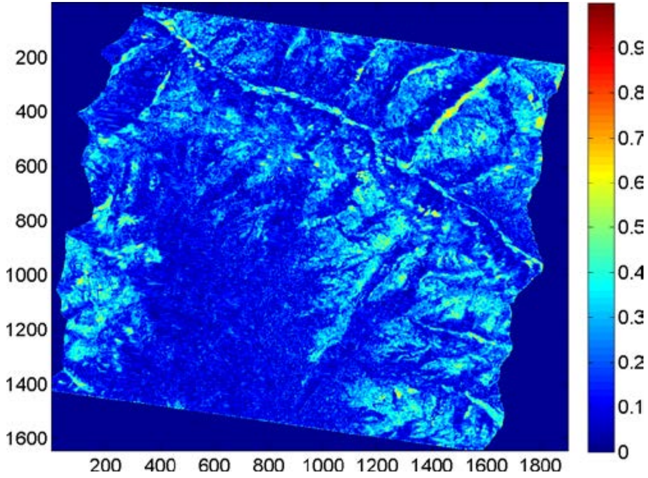

$GD(K_{Mar}, K_{Aug})_{HH-VV}$

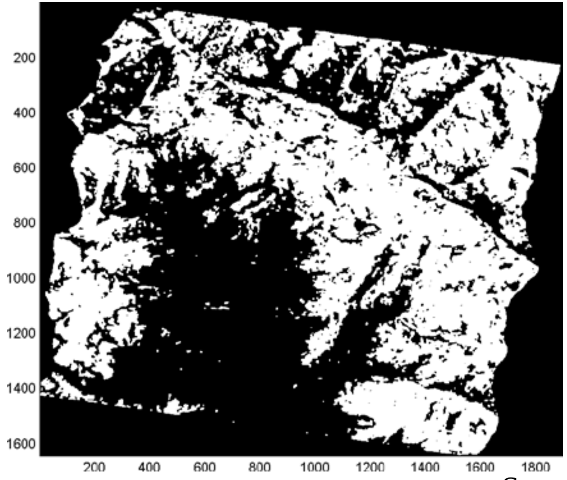

Snow Cover Map

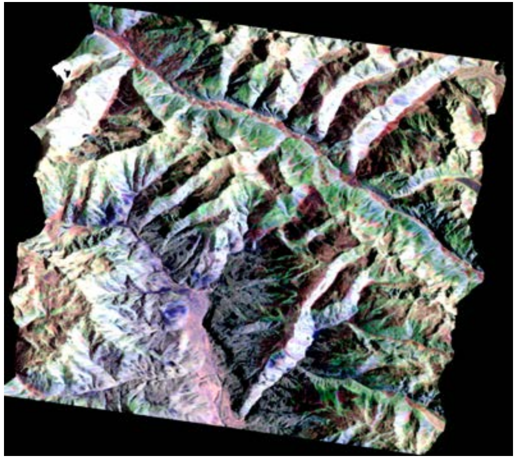

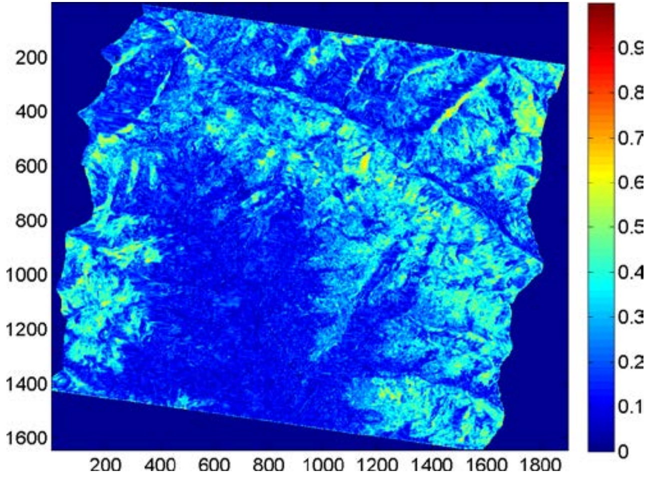

$GD(K_{Mar}, K_{Aug})_{FP}$

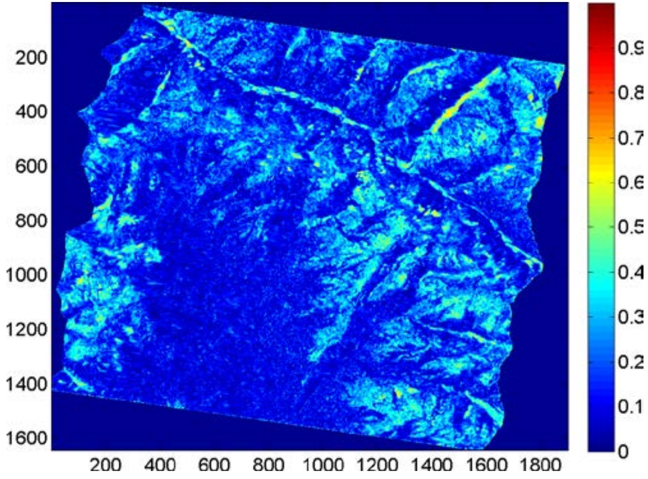

$GD(K_{Mar}, K_{Aug})_{HH-VV}$

Mar-Aug

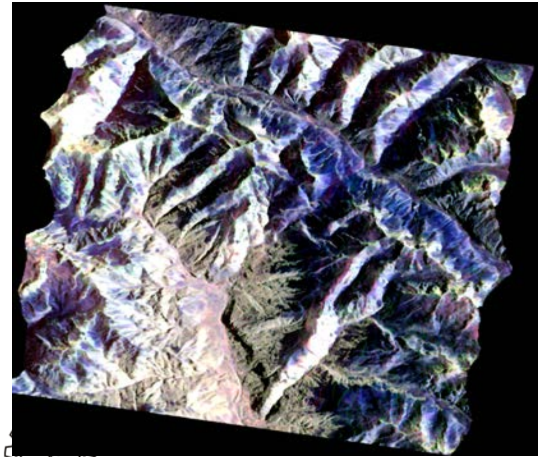

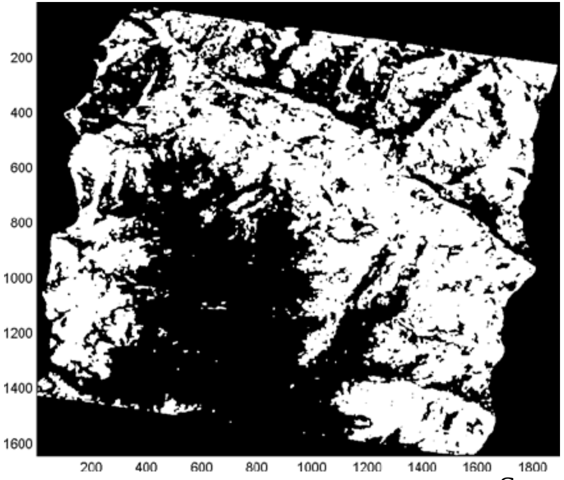

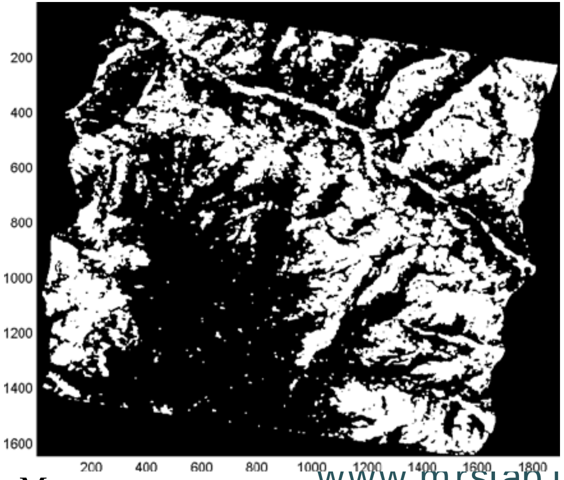

Snow Cover Map

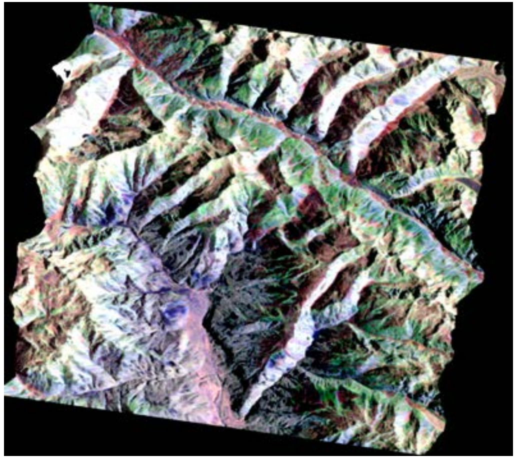

Mar-Aug

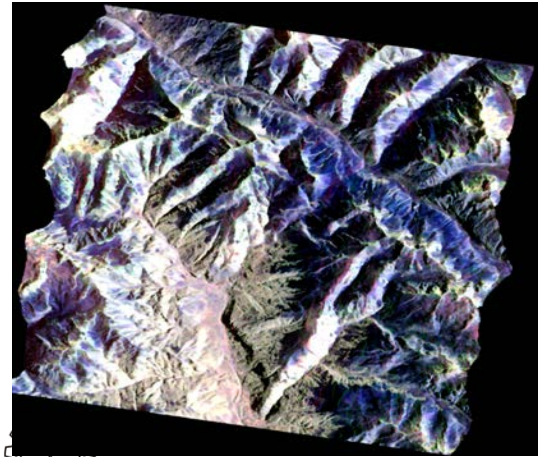

$GD(K_{Feb}, K_{Aug})_{HH-HV}$

$GD(K_{Feb}, K_{Aug})_{VV-HV}$

Snow Cover Map

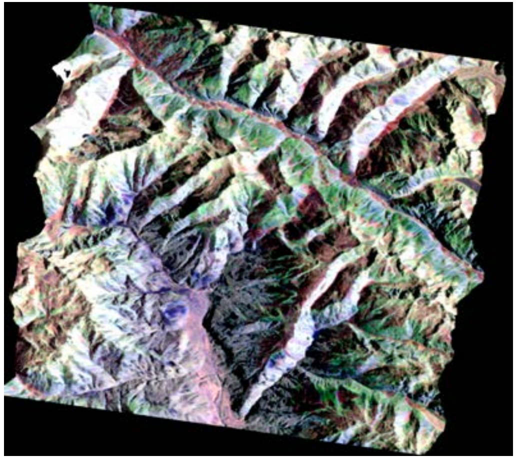

Mar-Aug

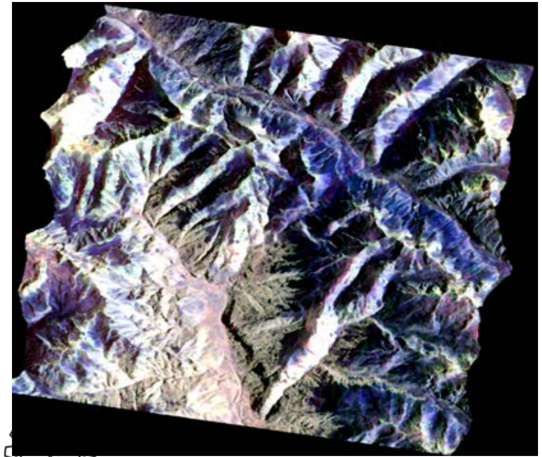

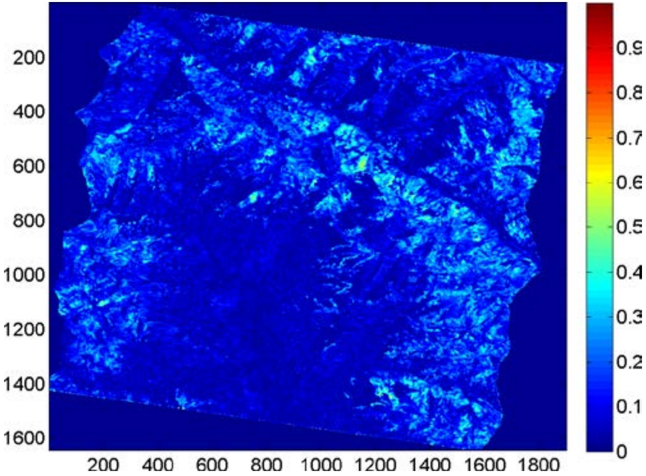

$GD(K_{Feb}, K_{Aug})_{HH-HV}$

$GD(K_{Feb}, K_{Aug})_{VV-HV}$

Snow Cover Map

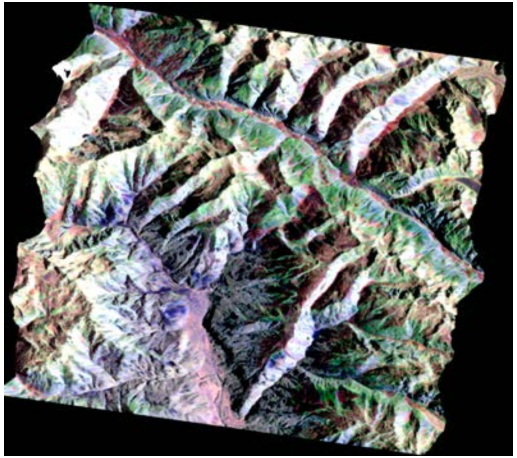

Mar-Aug

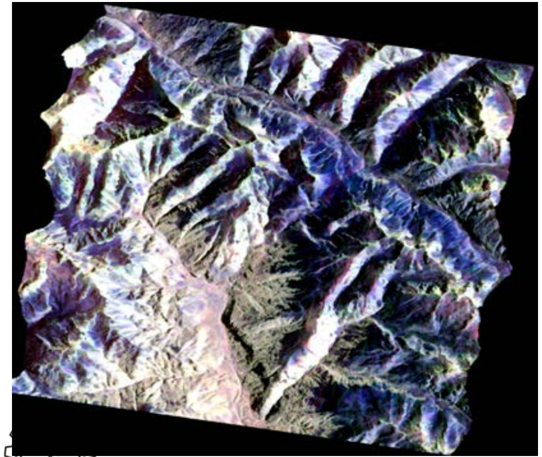

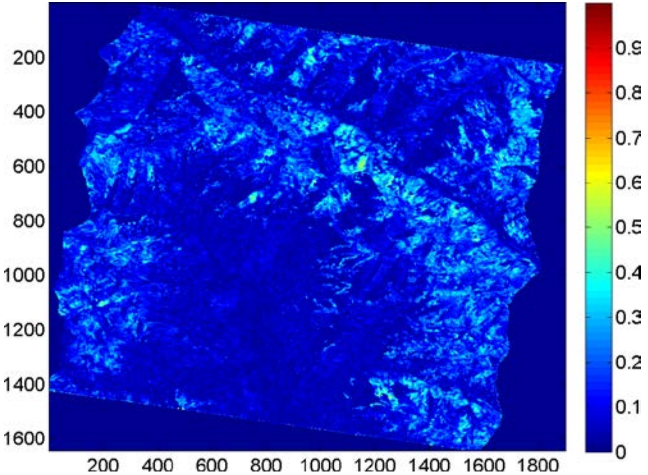

$GD(K_{Feb}, K_{Aug})_{HH-HV}$

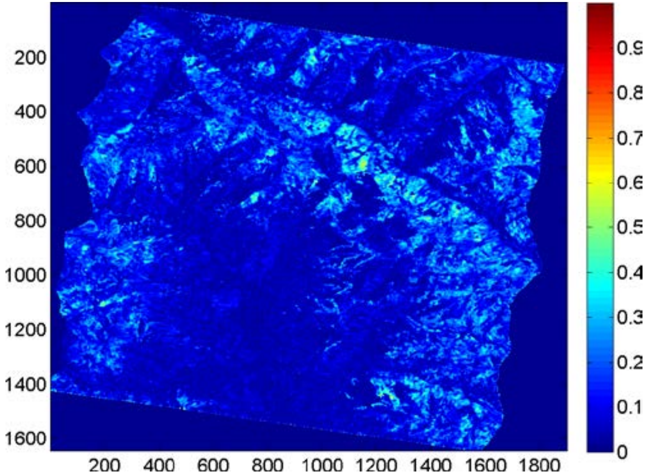

$GD(K_{Feb}, K_{Aug})_{VV-HV}$

Snow Cover Map

IIT Bombay

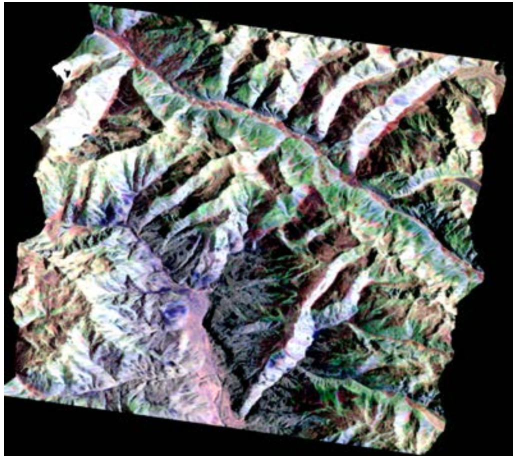

Mar-Aug

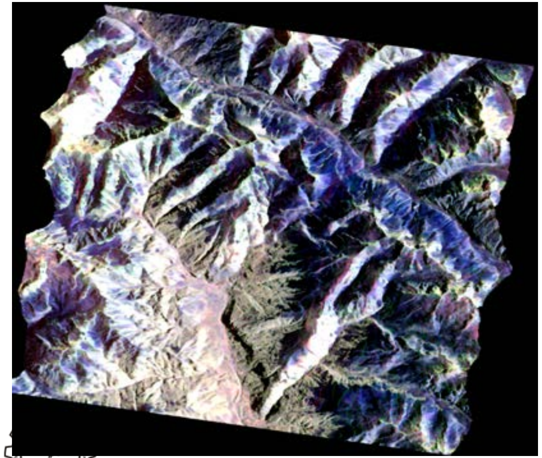

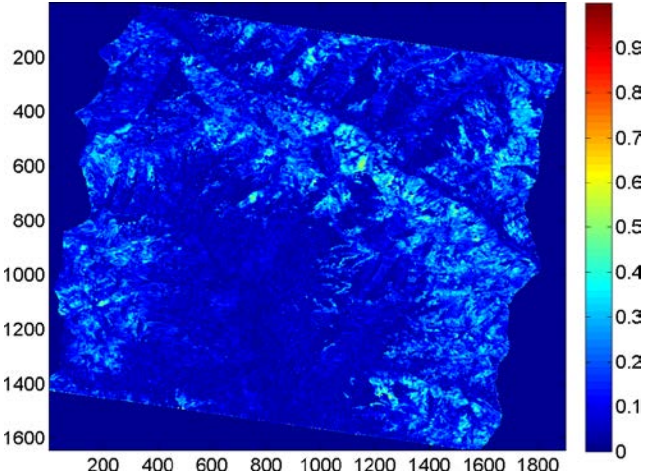

$GD(K_{Feb}, K_{Aug})_{HH-HV}$

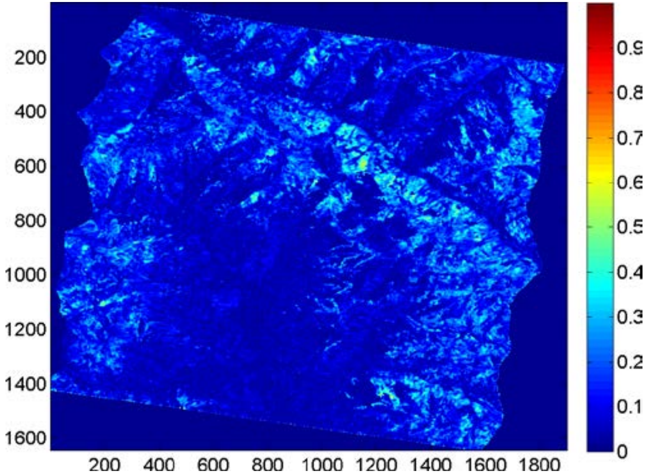

$GD(K_{Feb}, K_{Aug})_{VV-HV}$

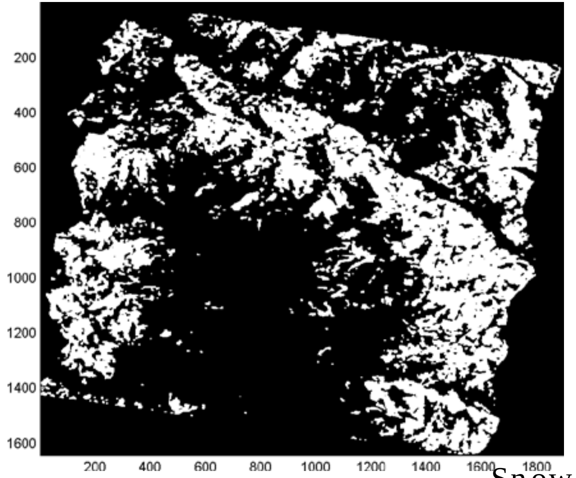

Snow Cover Map

IIT Bombay

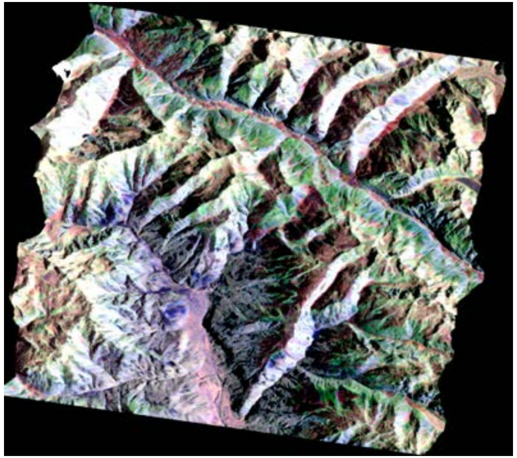

Mar-Aug

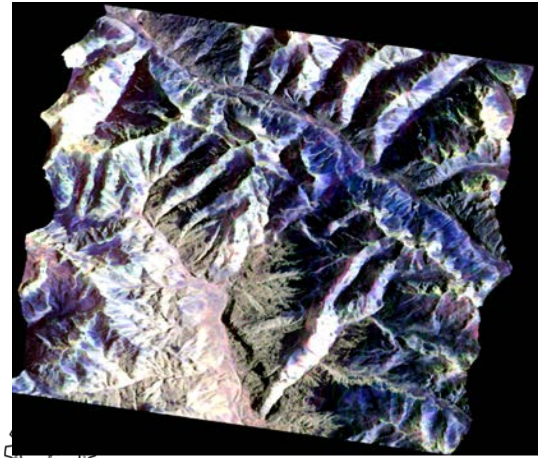

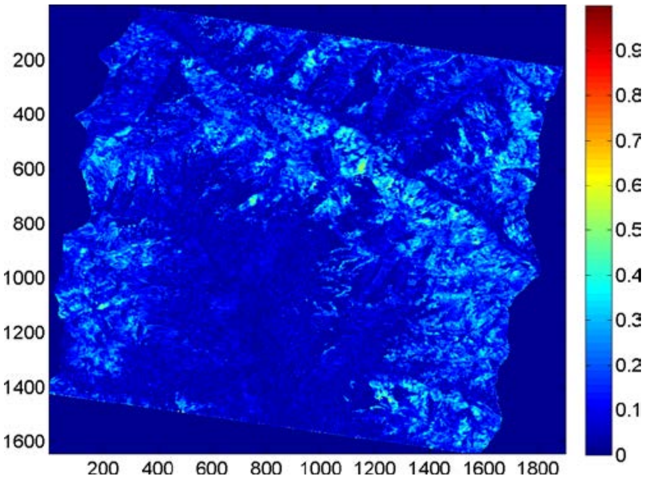

$GD(K_{Feb}, K_{Aug})_{HH-HV}$

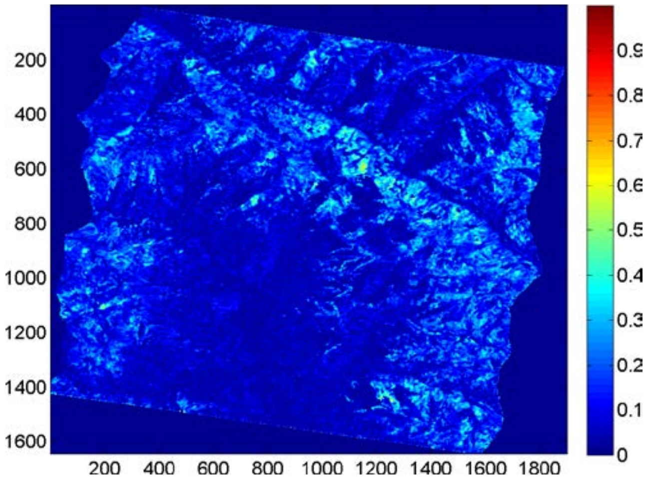

$GD(K_{Feb}, K_{Aug})_{VV-HV}$

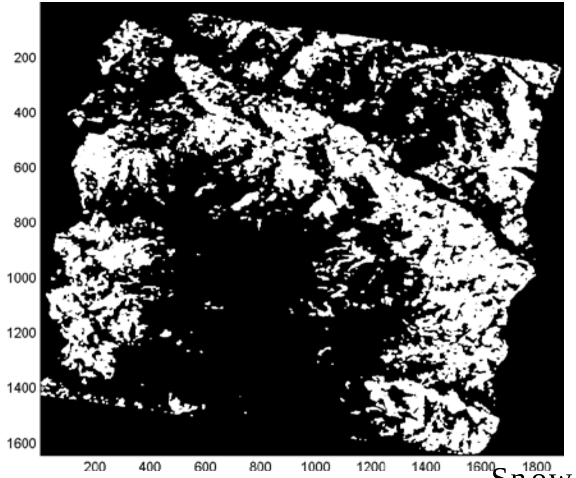

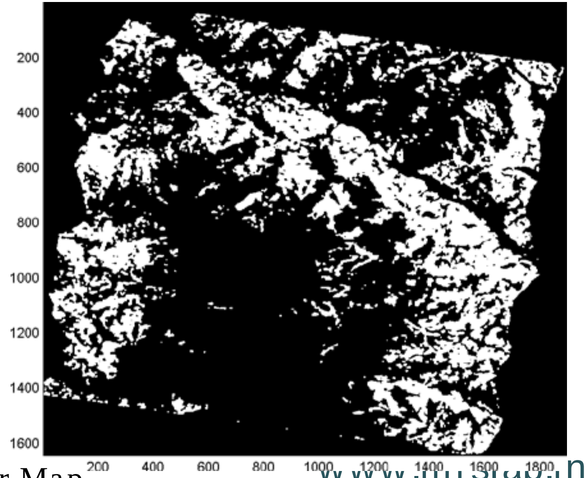

Snow Cover Map

FP

HH-VV

HH-HV

VV-VH

Snow Cover Map

IIT Bombay

FP

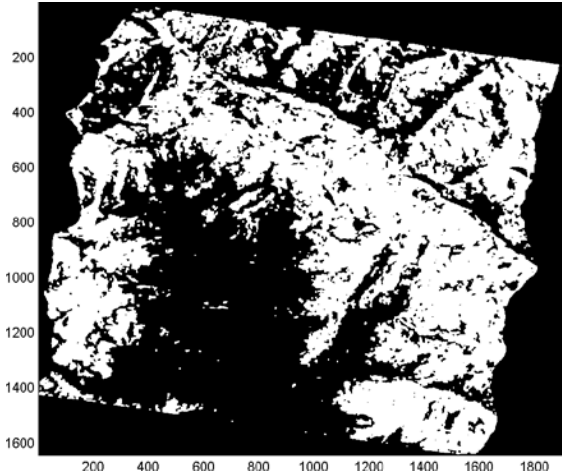

HH-VV

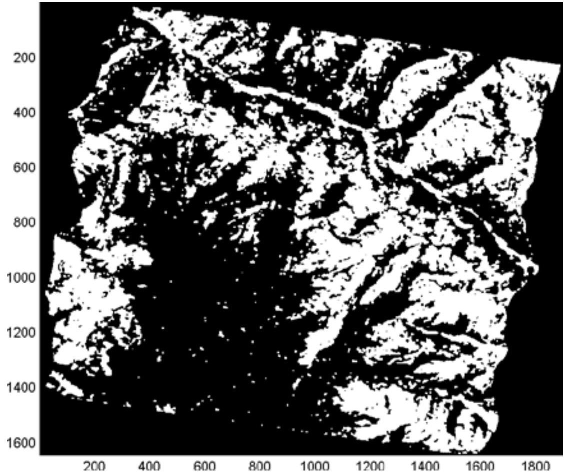

HH-HV

VV-VH

Snow Cover Map

FP

HH-VV

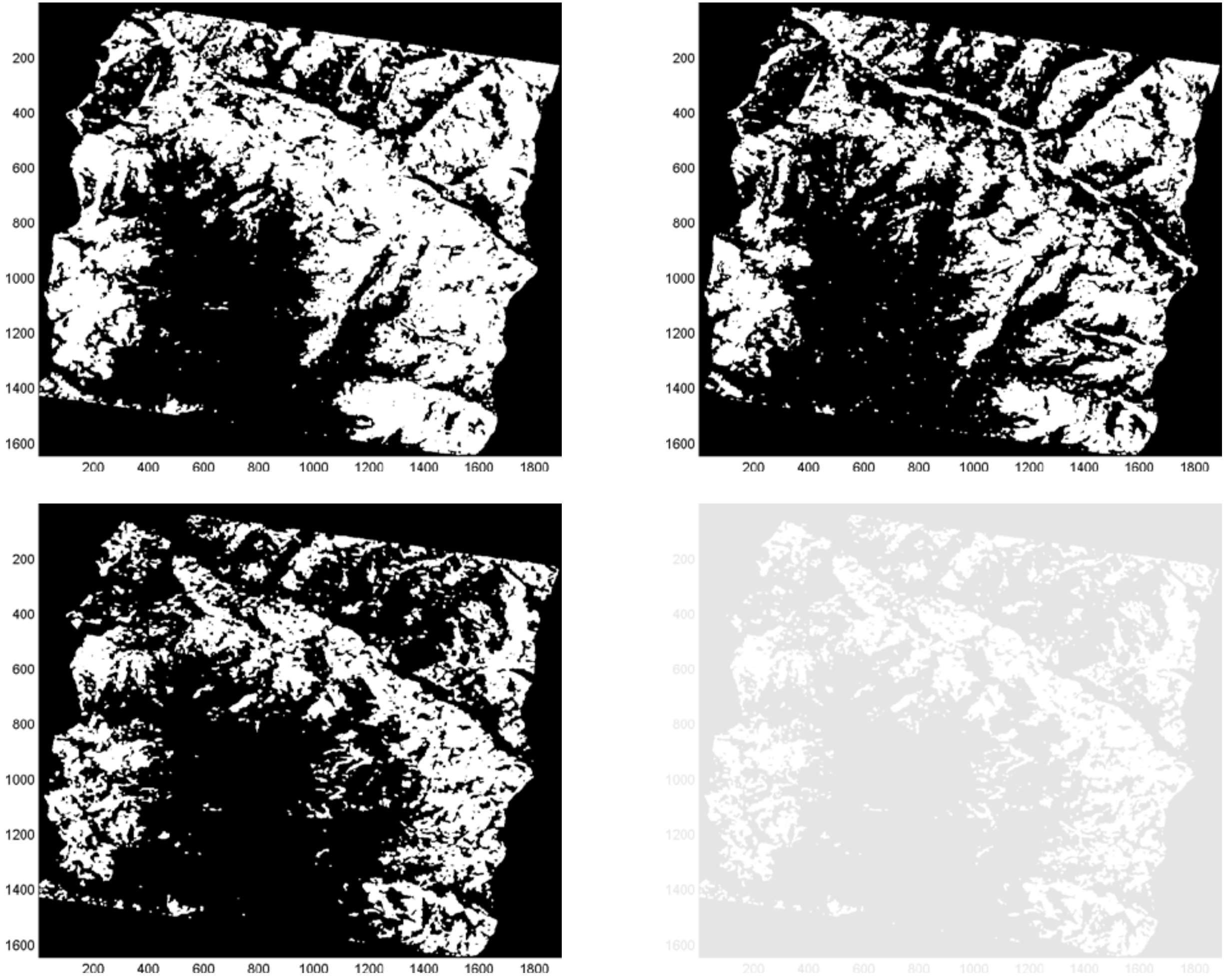

HH-HV

VV-VH

Snow Cover Map

FP

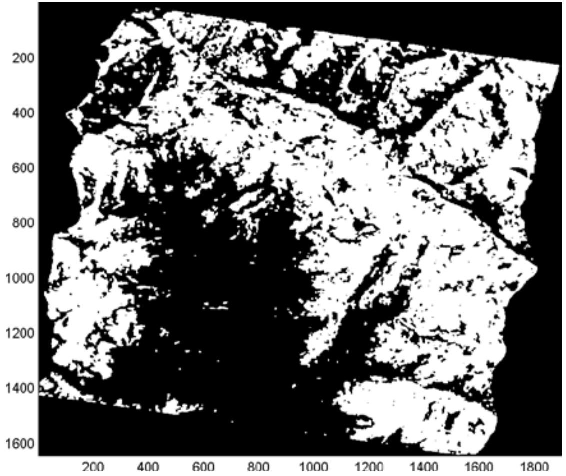

HH-VV

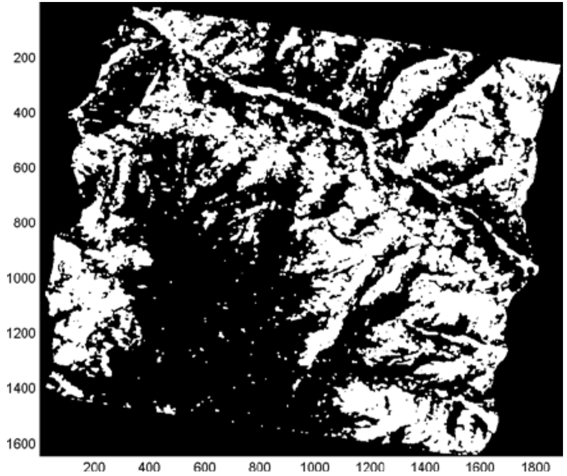

HH-HV

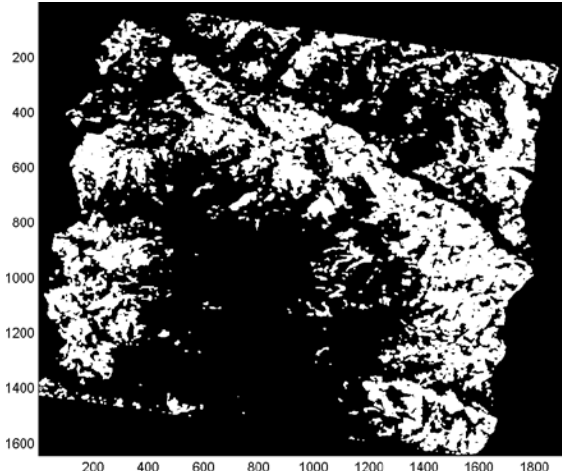

VV-VH

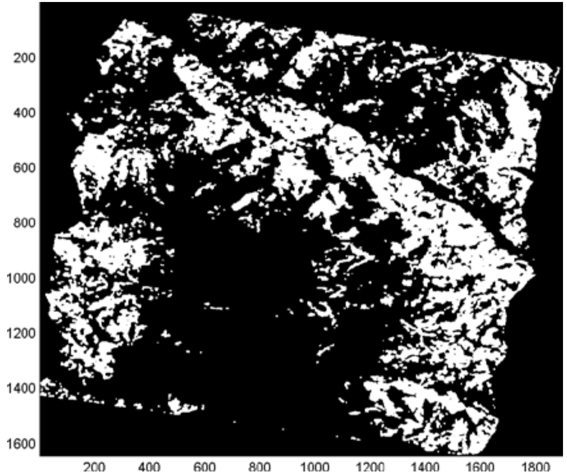

Snow Cover Map

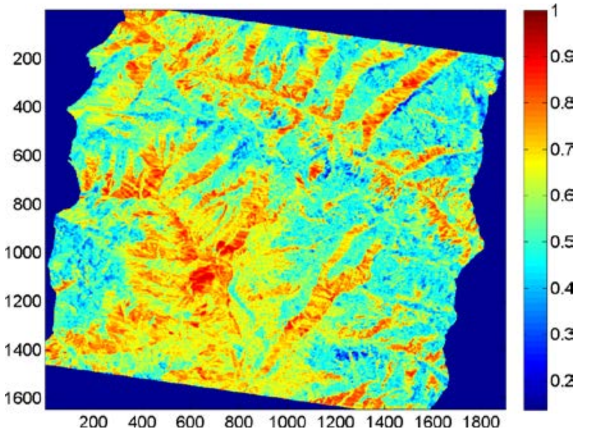

Feb. 2015: Trihedral Similarity

Mar. 2015: Trihedral Similarity

Aug. 2015: Trihedral Similarity

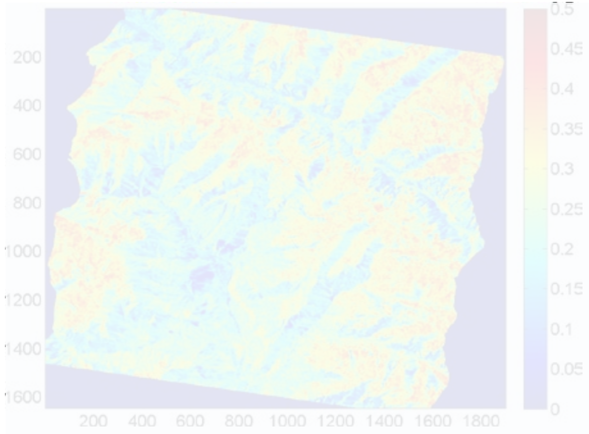

Feb. 2015: Helix Similarity

Mar. 2015: Helix Similarity

Aug. 2015: Helix Similarity

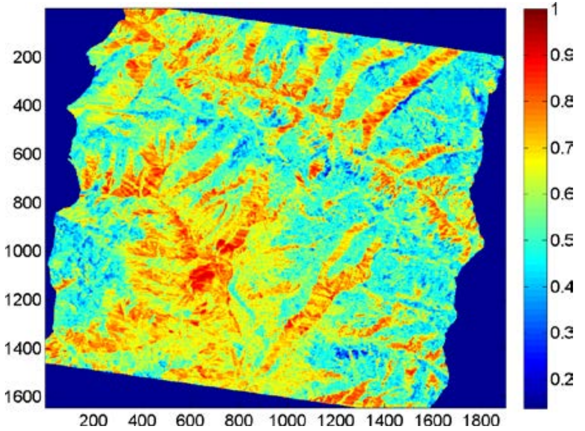

Feb. 2015: Trihedral Similarity

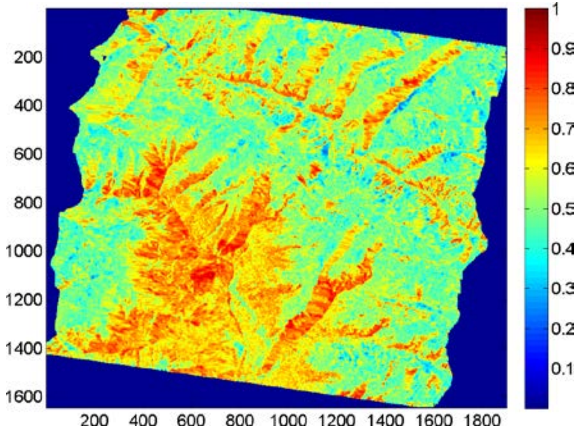

Mar. 2015: Trihedral Similarity

Aug. 2015: Trihedral Similarity

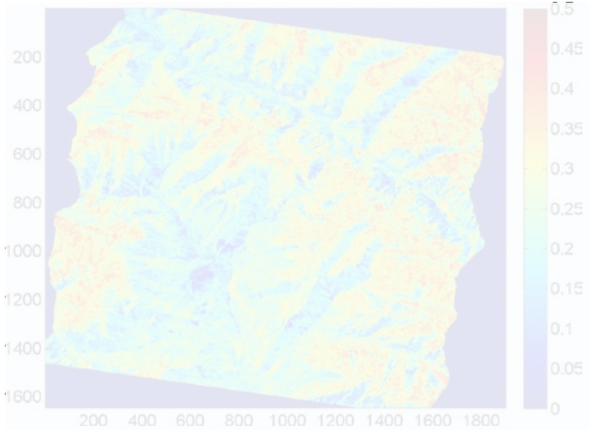
Feb. 2015: Helix Similarity

Mar. 2015: Helix Similarity

Aug. 2015: Helix Similarity

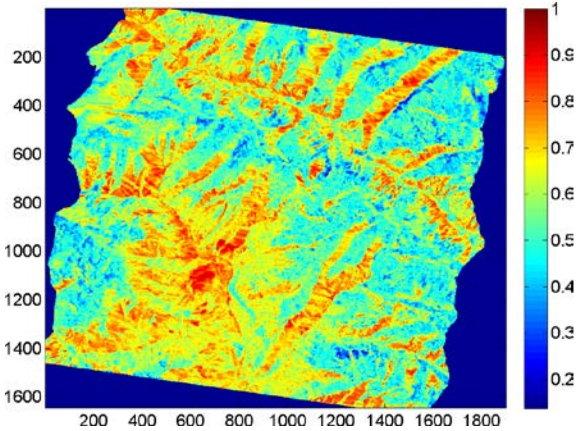

Feb. 2015: Trihedral Similarity

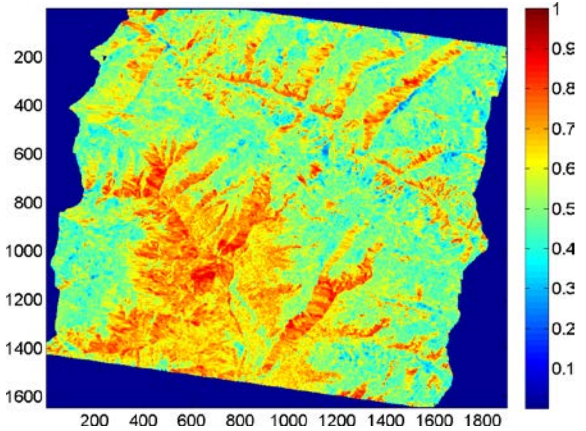

Mar. 2015: Trihedral Similarity

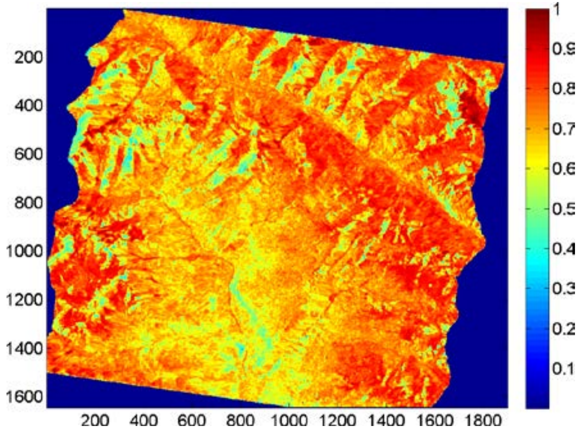

Aug. 2015: Trihedral Similarity

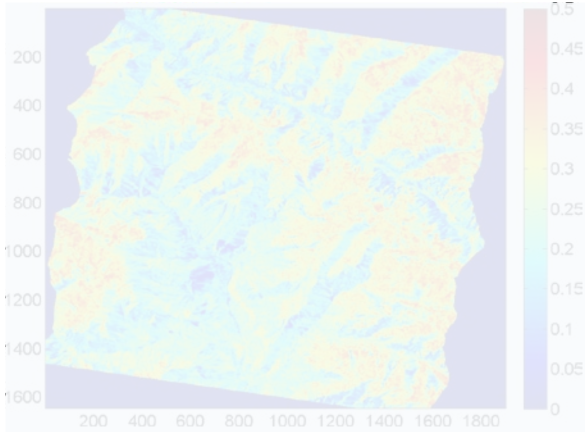

Feb. 2015: Helix Similarity

Mar. 2015: Helix Similarity

Aug. 2015: Helix Similarity

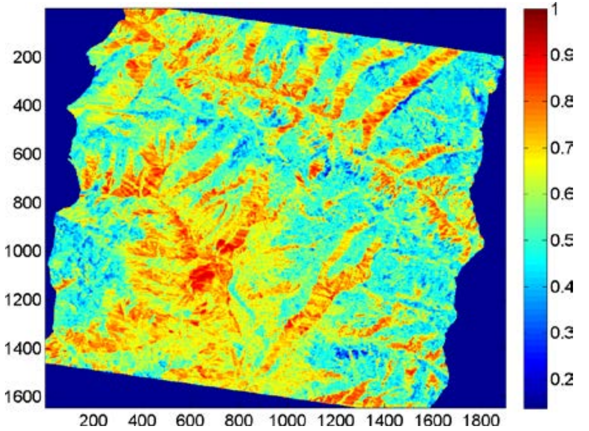

Feb. 2015: Trihedral Similarity

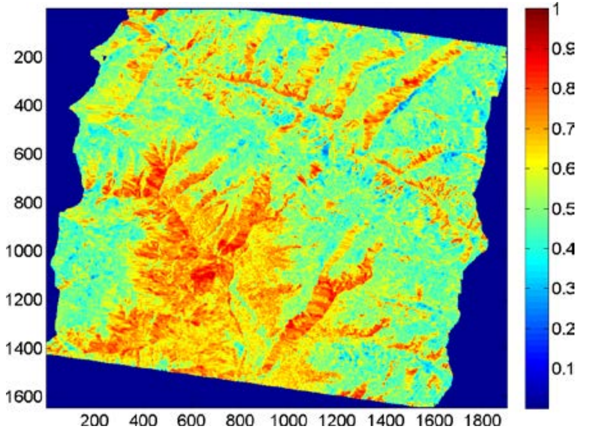

Mar. 2015: Trihedral Similarity

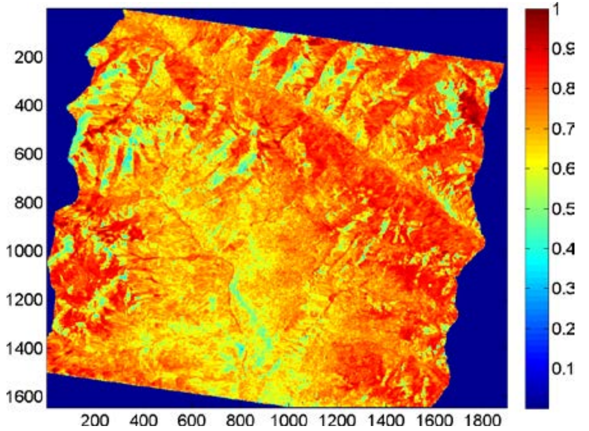

Aug. 2015: Trihedral Similarity

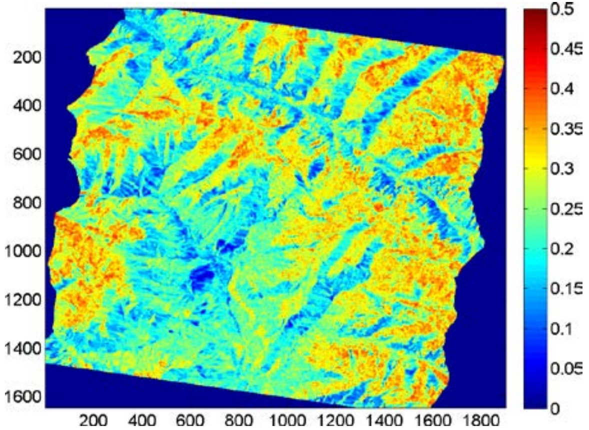

Feb. 2015: Helix Similarity

Mar. 2015: Helix Similarity

Aug. 2015: Helix Similarity

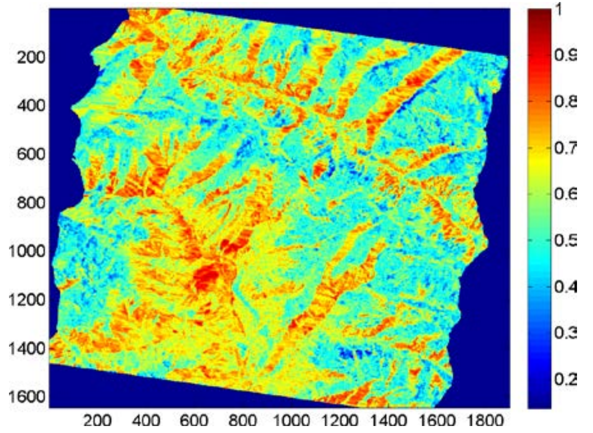

Feb. 2015: Trihedral Similarity

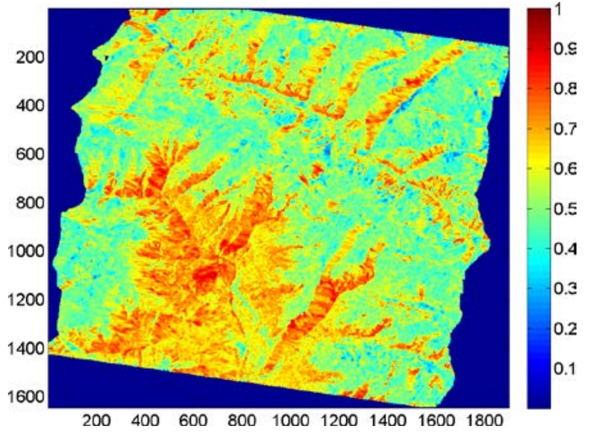

Mar. 2015: Trihedral Similarity

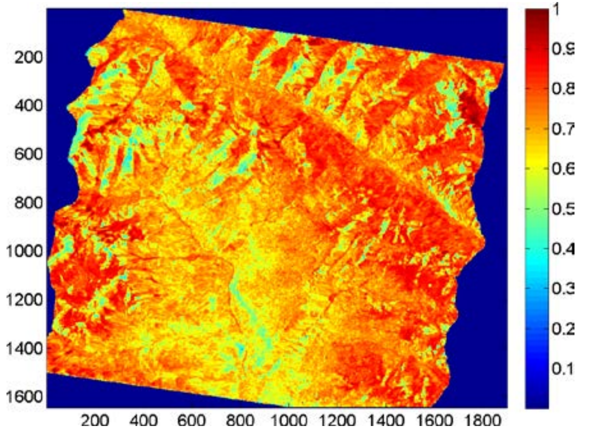

Aug. 2015: Trihedral Similarity

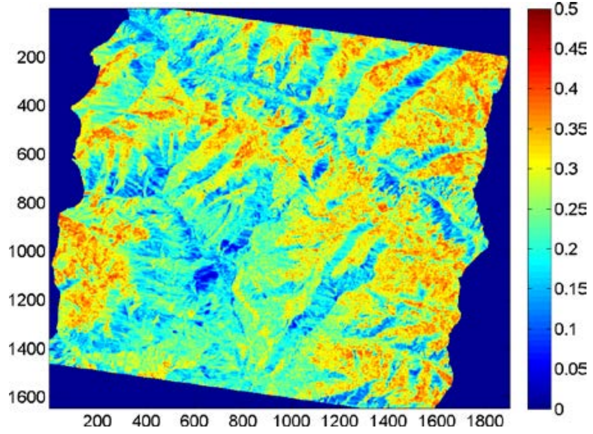

Feb. 2015: Helix Similarity

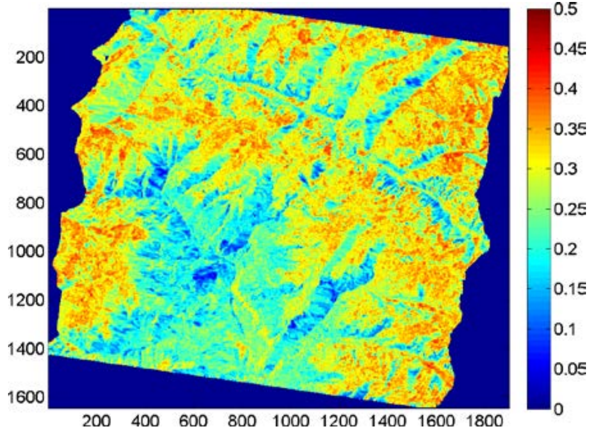

Mar. 2015: Helix Similarity

Aug. 2015: Helix Similarity

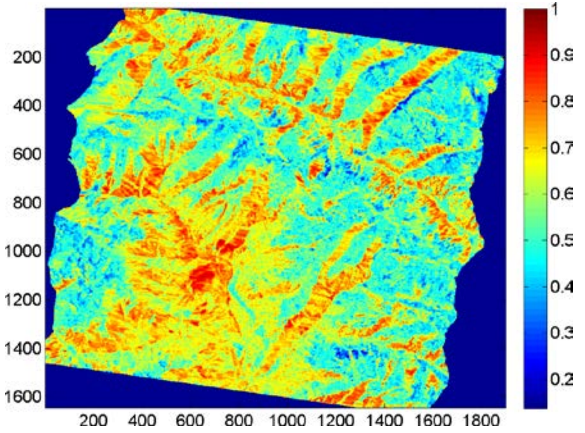

Feb. 2015: Trihedral Similarity

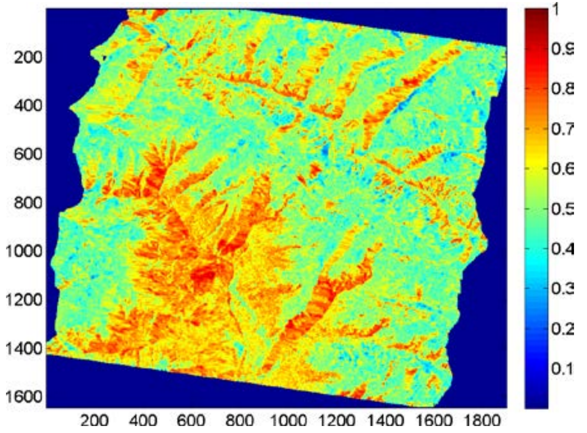

Mar. 2015: Trihedral Similarity

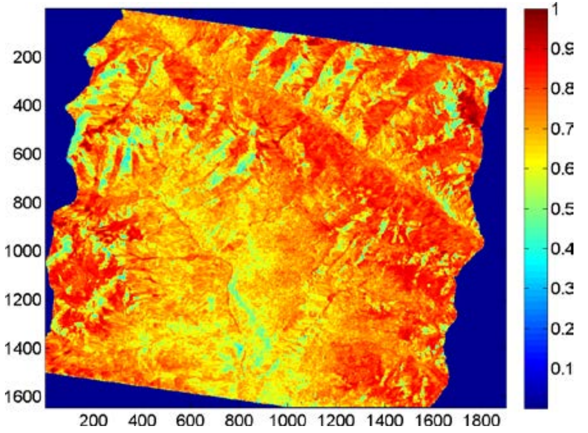

Aug. 2015: Trihedral Similarity

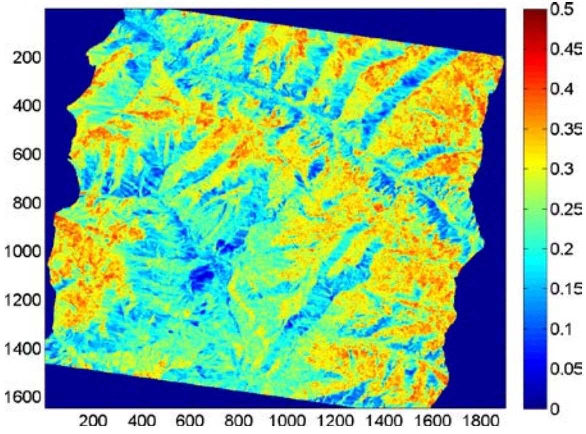

Feb. 2015: Helix Similarity

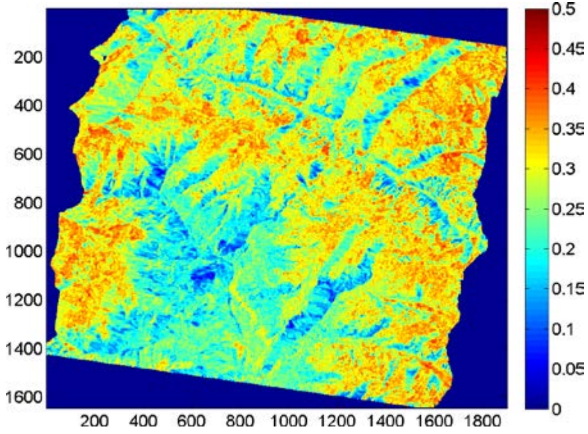

Mar. 2015: Helix Similarity

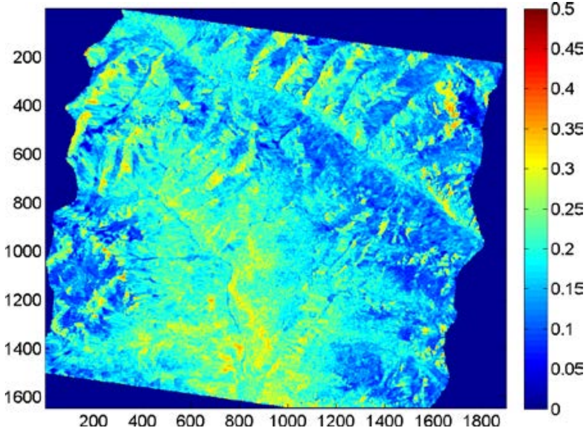

Aug. 2015: Helix Similarity

2

Scattering Mechanism Perspective

FRIEDRICH-ALEXANDER UNIVERSITÄT ERLANGEN-NÜRNBERG

IIT Bombay

Scattering Mechanisms

Bare Ground
Forest

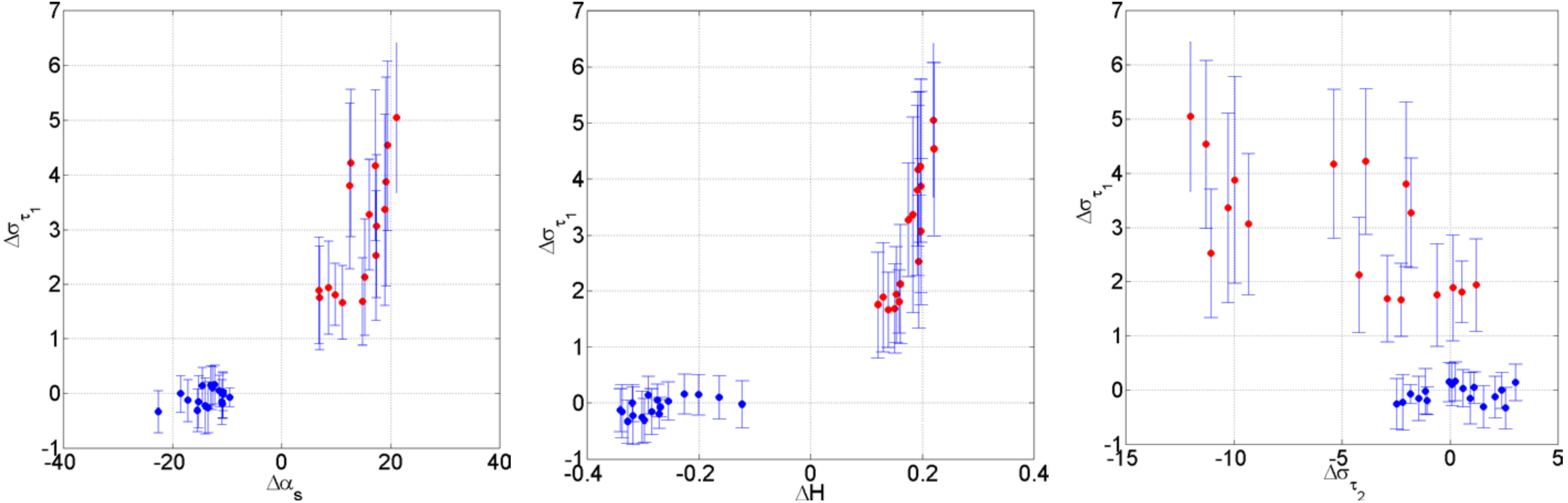

τ_1→ Describes the degree of helicity of the 1st dominant scattering mechanism
τ_2→ Describes the degree of helicity of the 2nd dominant scattering mechanism
α_s→ The scattering type magnitude
H → Quantifies the randomnessof the scattering mechanism

IIT Bombay

Scattering Mechanisms

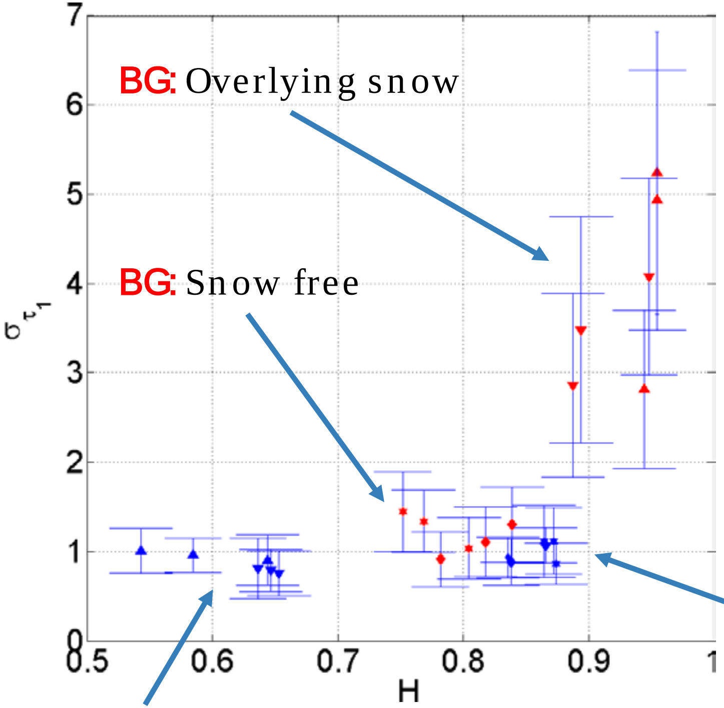

Bare Ground
Forest

- Notice that as snow disappeared over the Bare Ground (BG) the **Helicity variance** and the **Entropy** both **dropped**
- Thawing of Forest (F) resulted in **increase** in the **randomness** of scattering from those samples

IIT Bombay

Scattering Mechanisms

Early Morning Acquisition

Note the absence of snow over the canopy

Bare Ground (BG)

Snowpack froze overnight→ Dry snow volume enabled penetration of the incoming waves. Scattering is random due to interaction of the wave with complex snow matrix

Forest (F)

Freezing of moisture in vegetation→ Reduced complexity of scattering. Hence, low entropy scattering from forested areas

Scattering Mechanisms

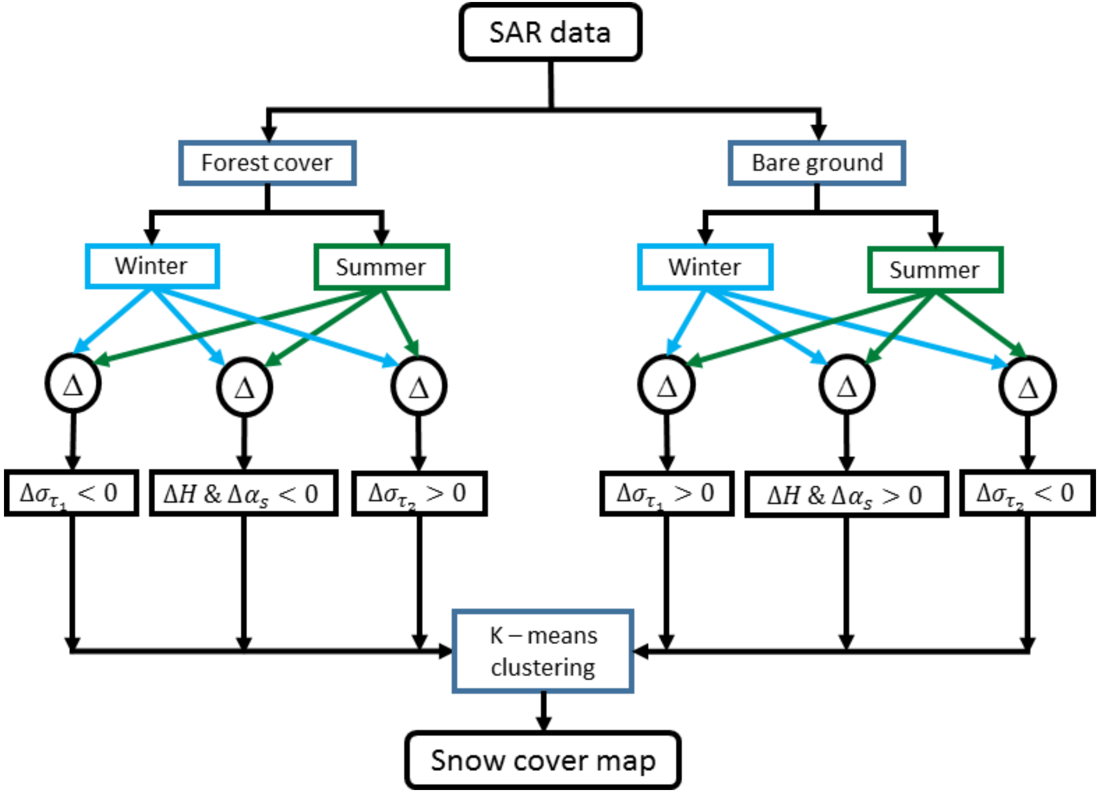

Scattering Mechanism Based Snow Cover Mapping Using RADARSAT-2 C-Band Polarimetric SAR Data,
A. Muhuri, S. Manickam and A. Bhattacharya, *IEEE Journal of Selected Topics in Applied Earth Observations and Remote Sensing*,
vol. 10, no. 7, pp. 3213-3224, 2017

Scattering Mechanisms

February

March

May

RADARSAT-2

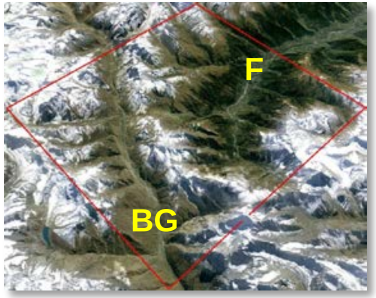

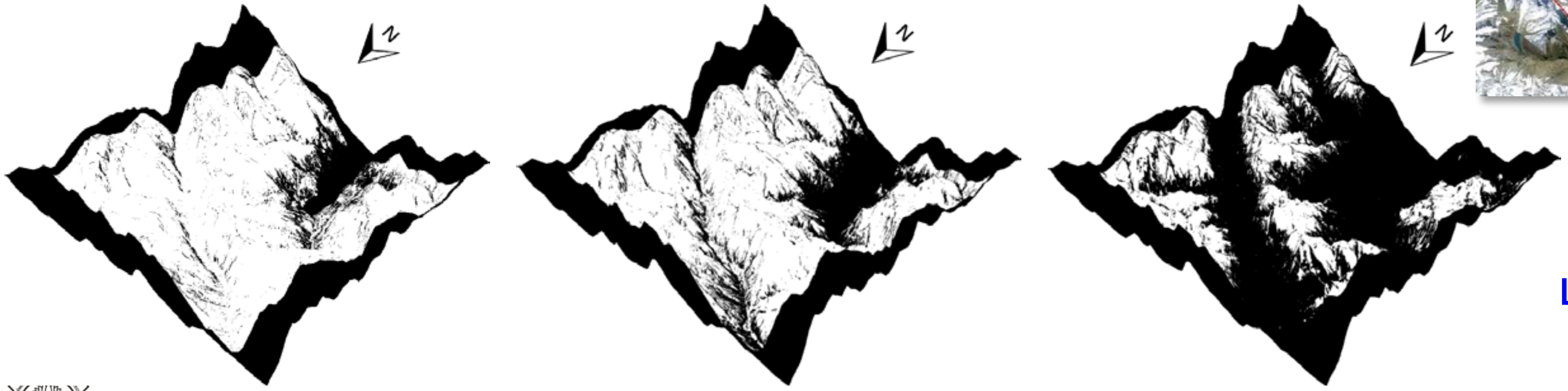

February

April

August

LANDSAT-8

3

Polarization Fraction Perspective

FRIEDRICH-ALEXANDER UNIVERSITÄT ERLANGEN-NÜRNBERG

IIT Bombay

$$\begin{bmatrix} E_H{}^{Scattered} \\ E_V{}^{Scattered} \end{bmatrix} = \begin{bmatrix} S_{HH} & S_{HV} \\ S_{VH} & S_{VV} \end{bmatrix} \begin{bmatrix} E_H{}^{Incident} \\ E_V{}^{Incident} \end{bmatrix}$$

Target Scattering Matrix

$$\Omega = \begin{bmatrix} S_{HH} & \sqrt{2}S_{HV} & S_{VV} \end{bmatrix}^T$$

Scattering Vector

$$C_3 = \langle \Omega.\Omega^{*T} \rangle = \begin{bmatrix} \langle |S_{HH}|^2 \rangle & \sqrt{2}\langle S_{HH}.S_{HV}^* \rangle & \langle S_{HH}.S_{VV}^* \rangle \\ \sqrt{2}\langle S_{HV}.S_{HH}^* \rangle & 2\langle |S_{HV}|^2 \rangle & \sqrt{2}\langle S_{HV}.S_{VV}^* \rangle \\ \langle S_{VV}.S_{HH}^* \rangle & \sqrt{2}\langle S_{VV}.S_{HV}^* \rangle & \langle |S_{VV}|^2 \rangle \end{bmatrix}$$

Covariance Matrix

$$\lambda_1 \geq \lambda_2 \geq \lambda_3$$

Eigenvalue spectrum conveys information about the diversity of the scattering mechanisms

$$\boxed{PF = 1 - \frac{3\lambda_3}{\lambda_1 + \lambda_2 + \lambda_3}}$$

Polarized Fraction

H/α Segmentation

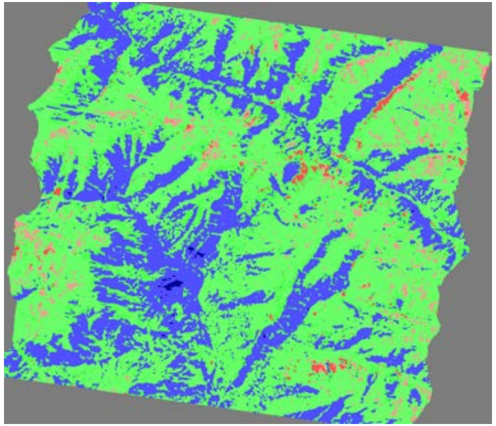

Feb. 2015

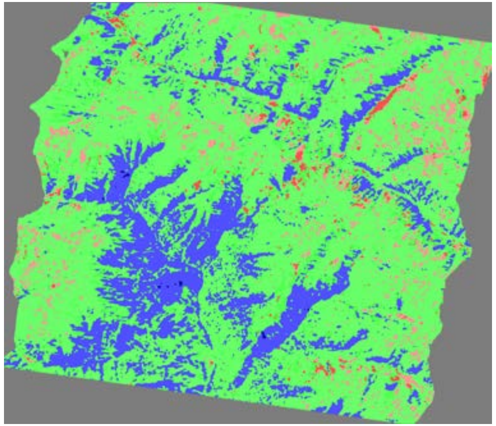

Mar. 2015

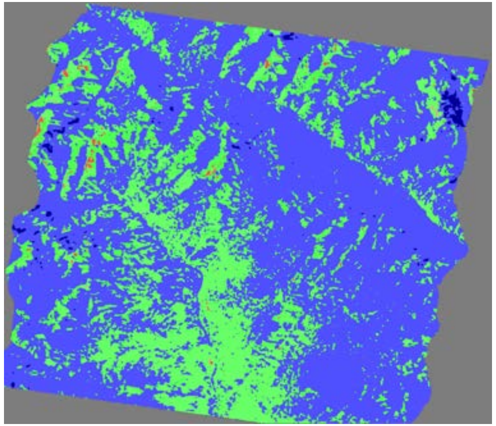

Aug. 2015

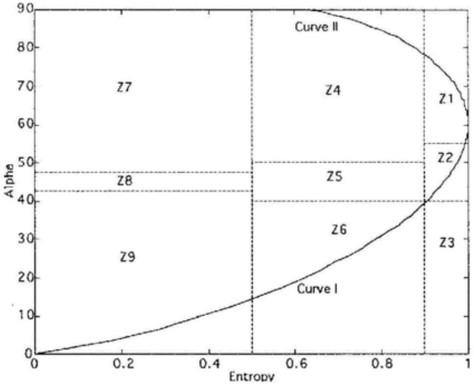

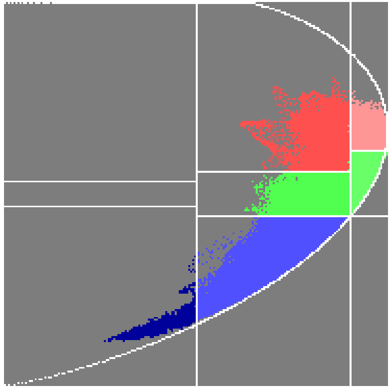

Feb. 2015

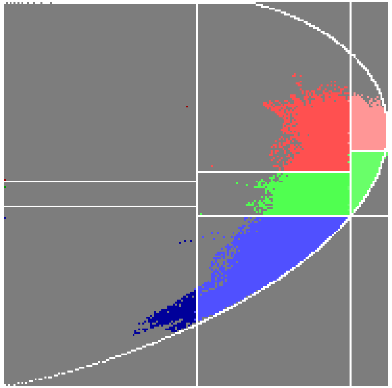

Mar. 2015

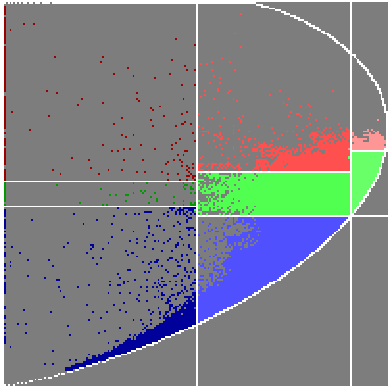

Aug. 2015

IIT Bombay

Polarization Fraction Perspective

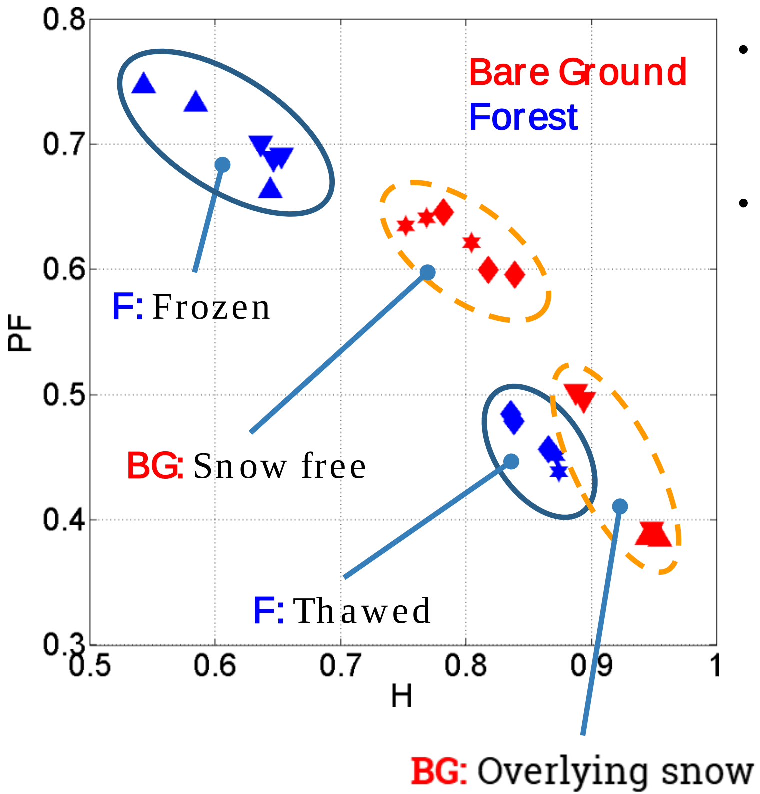

- Frozen Forest (F) demonstrated substantially Polarized Return as compared to Bare Ground (BG) with overlying snow where Unpolarized Return was evident with Randomness in Scattering
- As snow cover disappeared beyond March and Minimum Temperature crossed the 0^0C line, the returns from BG areas were comparatively more Polarized than those belonging to the F class

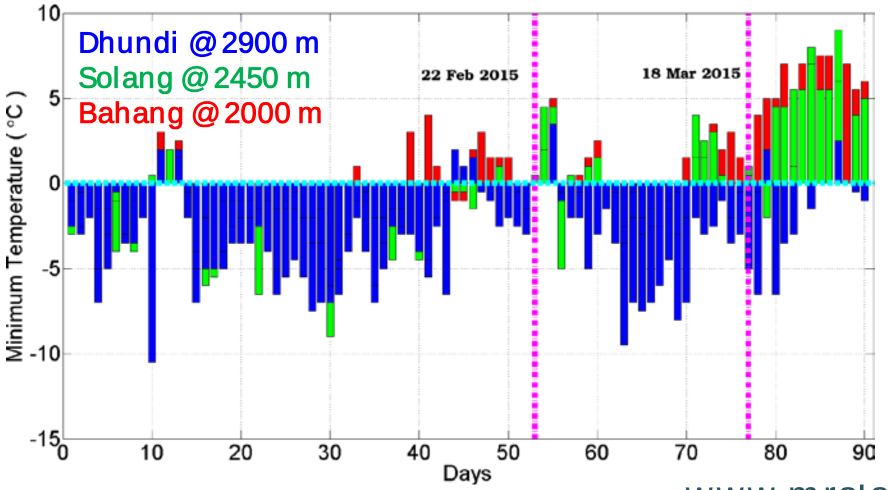

IIT Bombay

Polarization Fraction Perspective

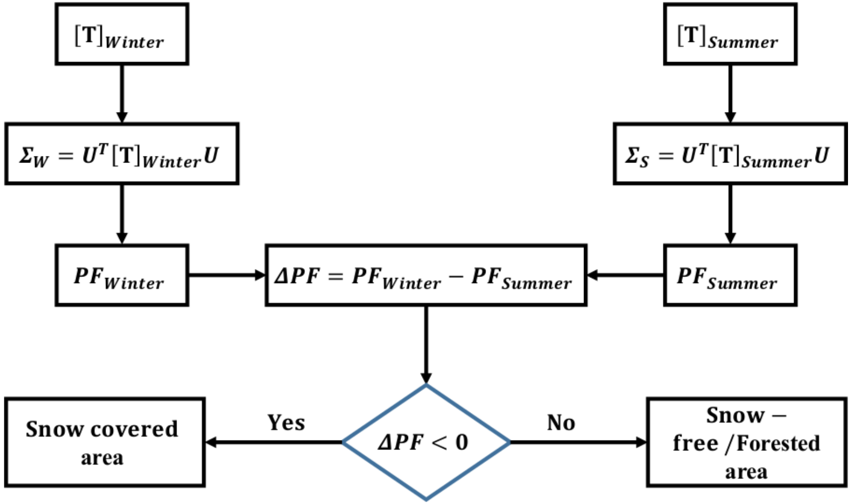

Proposed flowchart

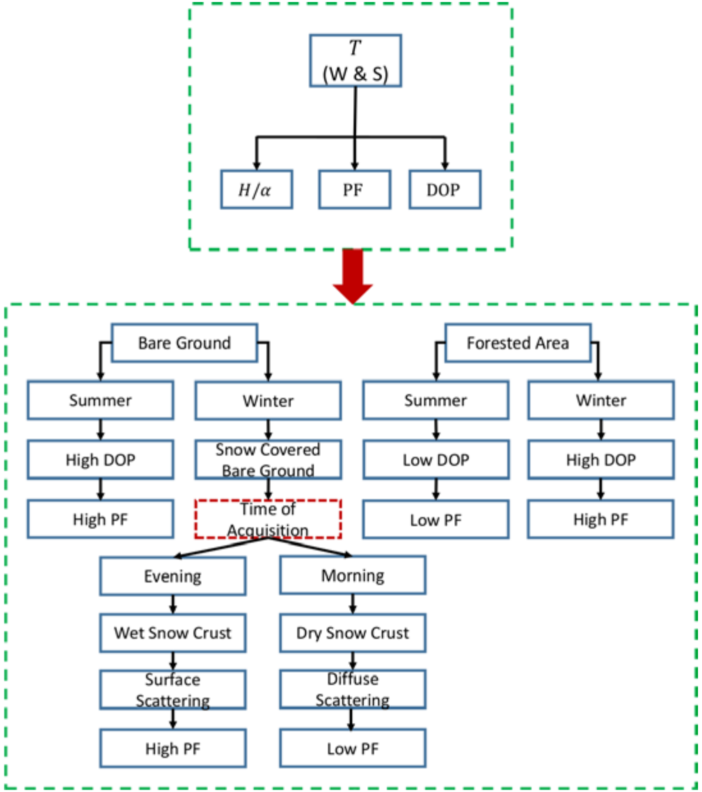

Seasonal response of polarimetric indicators

Snow Cover Mapping Using Polarization Fraction Variation With Temporal RADARSAT-2 C-Band Full-Polarimetric SAR Data Over the Indian Himalayas, A. Muhuri, S. Manickam and A. Bhattacharya, Snehmani, *IEEE Journal of Selected Topics in Applied Earth Observations and Remote Sensing*, vol. 11, no. 7, pp. 2192-2209, 2018

Polarization Fraction Perspective

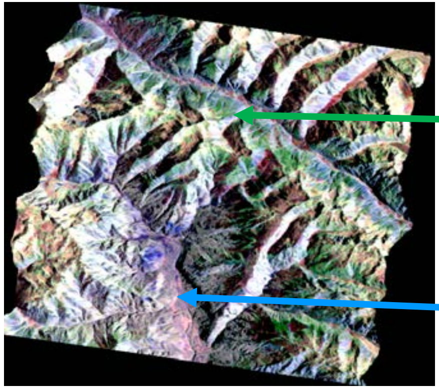

February

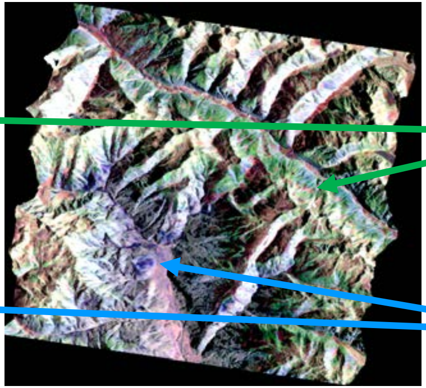

March

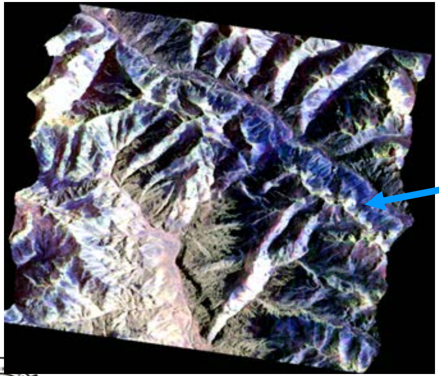

May

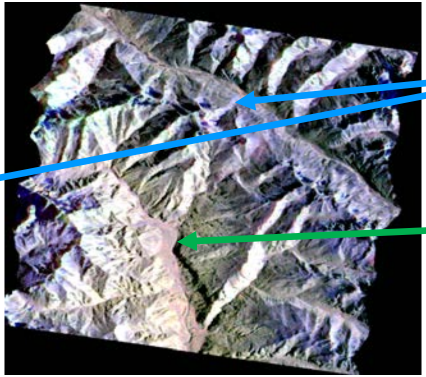

August

Notice the dominance of volume scattering in the month of February & March from snow covered areas situated above the mean tree line

Notice the dominance of surface scattering in the month of February & March from forested areas situated below the mean tree line

Surface scattering is restored with the disappearance of snow cover from the barren areas

Volume scattering begins to predominates over the forested areas with the onset of summer

Polarization Fraction Perspective

RADARSAT-2

February

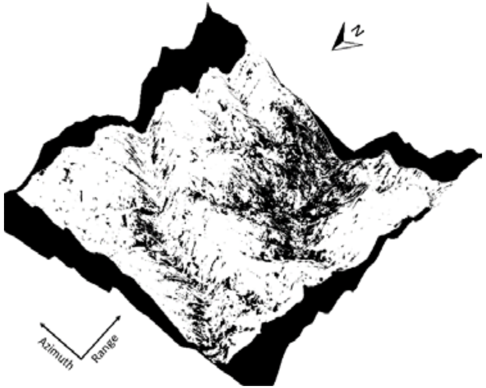

March

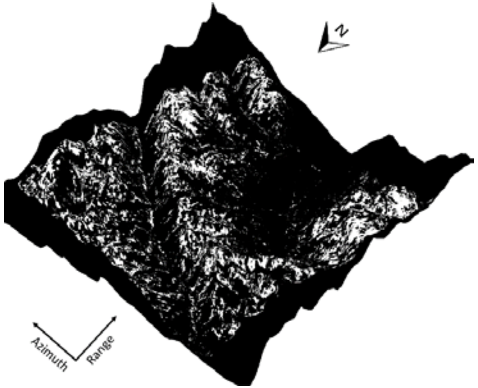

May

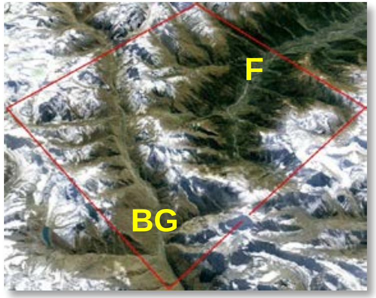

February

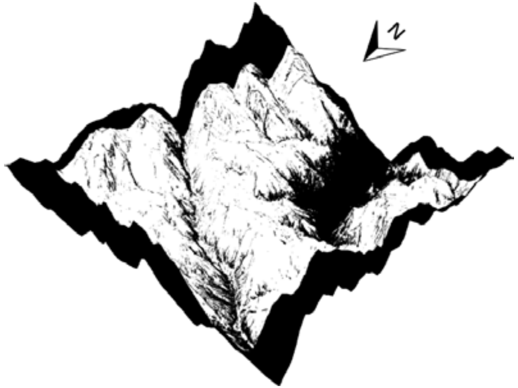

April

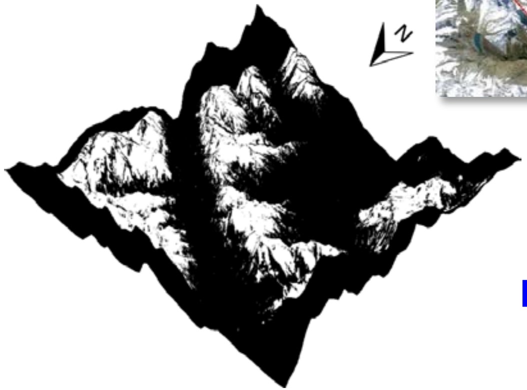

August

LANDSAT-8

4

Polarimetric Channel Correlation Perspective

IIT Bombay

Polarimetric Channel Correlation Perspective

$$\begin{bmatrix} E_H{}^{Scattered} \\ E_V{}^{Scattered} \end{bmatrix} = \begin{bmatrix} S_{HH} & S_{HV} \\ S_{VH} & S_{VV} \end{bmatrix} \begin{bmatrix} E_H{}^{Incident} \\ E_V{}^{Incident} \end{bmatrix}$$

Target Scattering Matrix

$$\Omega = \begin{bmatrix} S_{HH} & \sqrt{2}S_{HV} & S_{VV} \end{bmatrix}^T$$

Scattering Vector

$$C_3 = \langle \Omega.\Omega^{*T} \rangle = \begin{bmatrix} \langle |S_{HH}|^2 \rangle & \sqrt{2}\langle S_{HH}.S_{HV}^* \rangle & \langle S_{HH}.S_{VV}^* \rangle \\ \sqrt{2}\langle S_{HV}.S_{HH}^* \rangle & 2\langle |S_{HV}|^2 \rangle & \sqrt{2}\langle S_{HV}.S_{VV}^* \rangle \\ \langle S_{VV}.S_{HH}^* \rangle & \sqrt{2}\langle S_{VV}.S_{HV}^* \rangle & \langle |S_{VV}|^2 \rangle \end{bmatrix}$$

Covariance Matrix

Polarimetric Channel Correlation Perspective

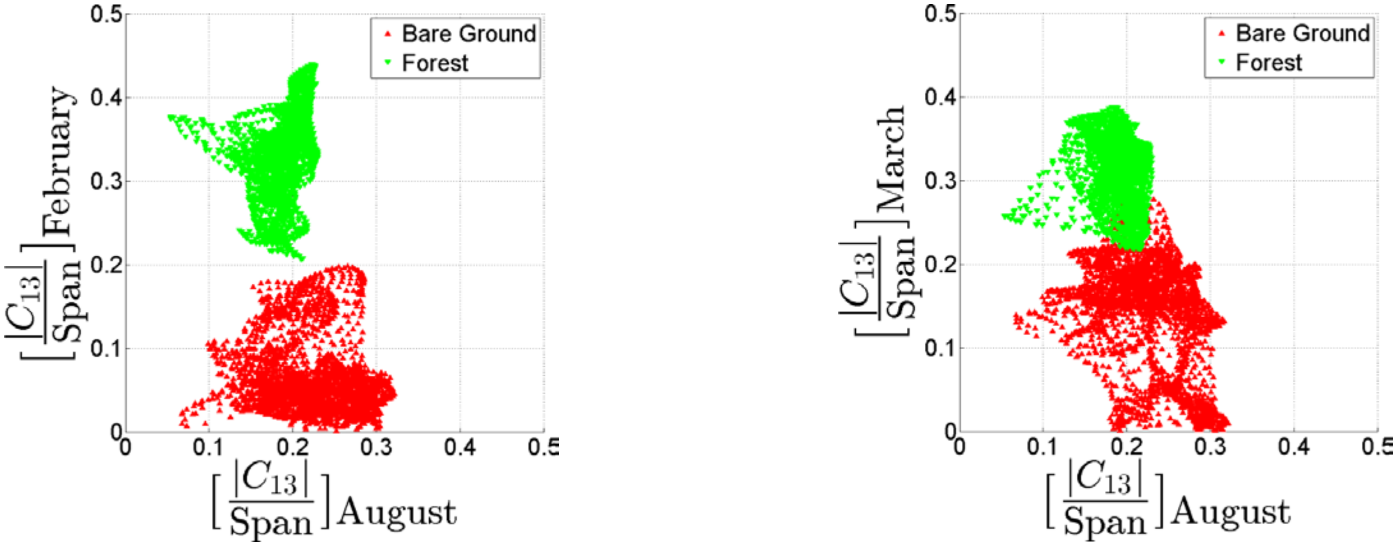

$$\Gamma = \frac{|C_{13}|}{\text{Span}} \qquad \Delta = 10 \cdot \log_{10}\left[\frac{\Gamma_{winter}}{\Gamma_{summer}}\right]$$

$$\text{Span} = C_{11} + C_{22} + C_{33}$$

Δ image is thresholded using the method of Otsu

IIT Bombay

Seasonal Snow Cover Change Detection Over the Indian Himalayas Using Polarimetric SAR Images,,
A. Muhuri, D. Ratha and A. Bhattacharya, *IEEE Geoscience and Remote Sensing Letters*, vol. 14, no. 12, pp. 2192-2209, 2017

Polarimetric Channel Correlation Perspective

RADARSAT-2

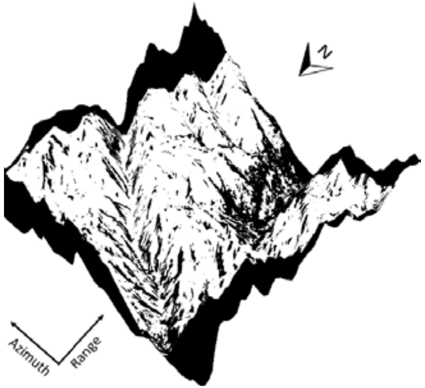

February

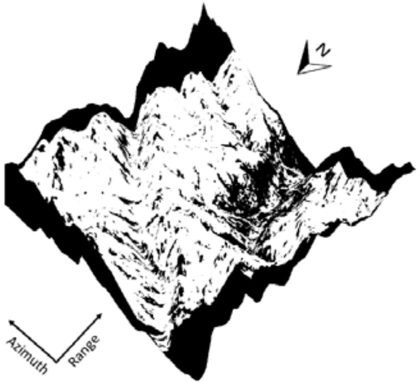

March

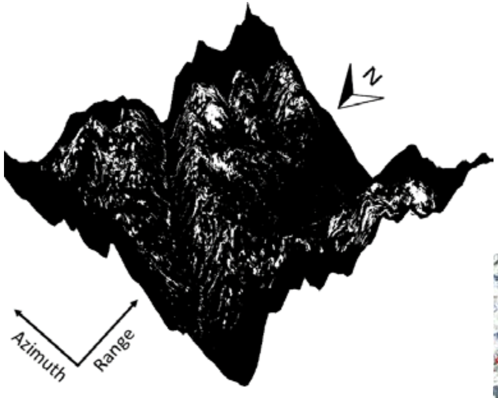

May

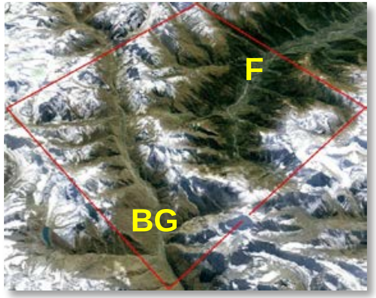

February

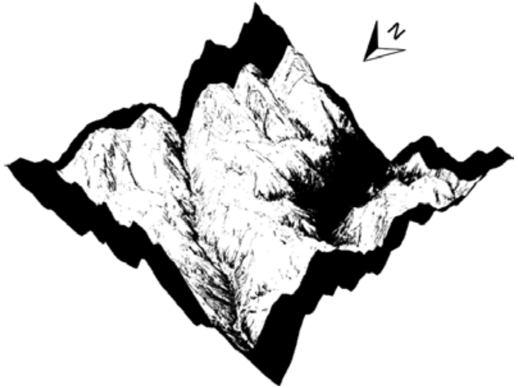

April

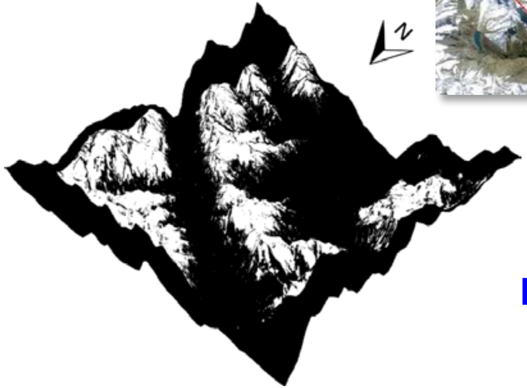

August

LANDSAT-8

5

General Polarization Basis + Deep Learning

IIT Bombay

Poincaré Sphere Parameters

Transformation of the **Stokes vector** to any **general polarization basis** using the Kennaugh $\langle[\mathbf{K}]\rangle$ matrix as:

$$\begin{bmatrix} g_{0r} \\ g_{1r} \\ g_{2r} \\ g_{3r} \end{bmatrix} = \langle[\mathbf{K}]\rangle \cdot \begin{bmatrix} g_{0i} \\ g_{1i} \\ g_{2i} \\ g_{3i} \end{bmatrix}$$

g_i	H	V	R	L	General
g_{0i}	1	1	1	1	1
g_{1i}	1	-1	0	0	$\cos(2\psi)\cos(2\tau)$
g_{2i}	0	0	0	0	$\sin(2\psi)\cos(2\tau)$
g_{3i}	0	0	-1	1	$\sin(2\tau)$

Special Cases:

Circular (L) Basis: $\psi = 0°, \tau = 45°$

Linear (H) Basis: $\psi = 0°, \tau = 0°$

$\pi/4$ Basis: $\psi = 45°, \tau = 0°$

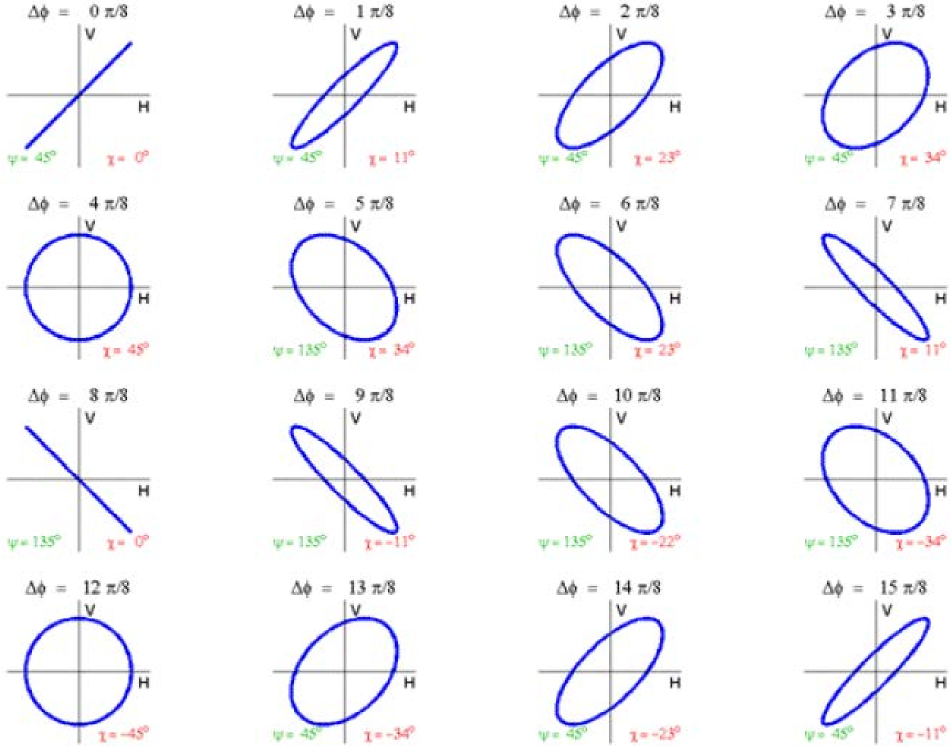

Wave Polarization Basis

Overall Methodology

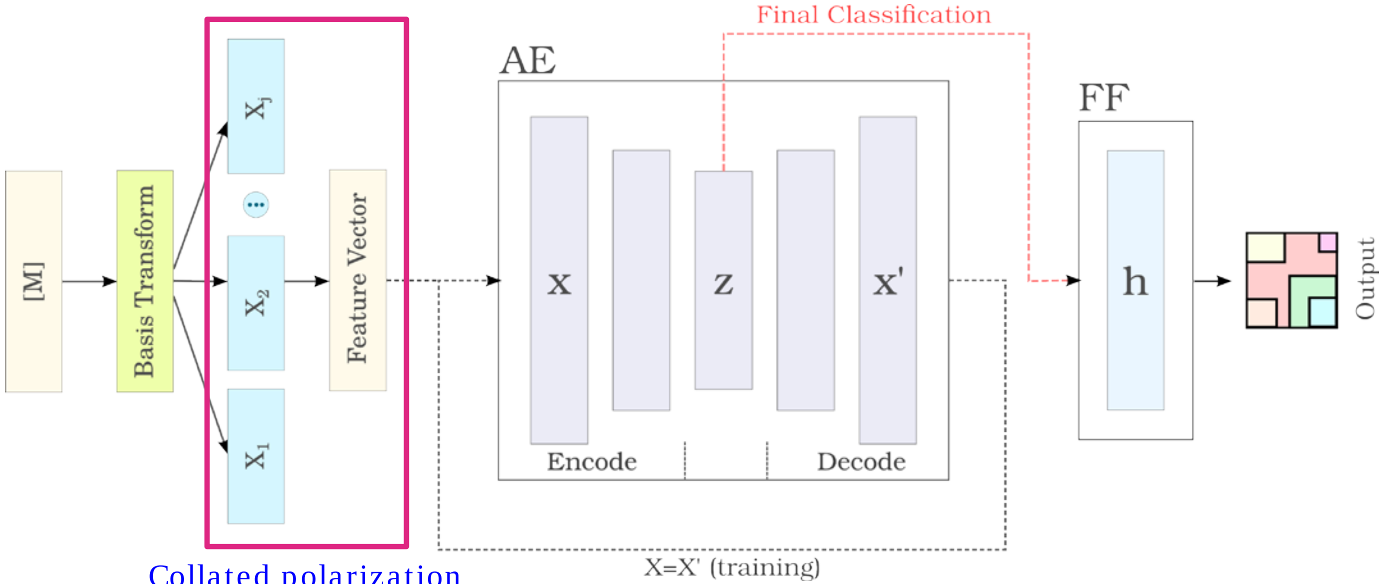

Collated polarization basis transformed Stokes parameters

$$X_j = \left[\, g_{0r}\ \bar{\mathbf{g}}_{\mathbf{1r_i}}\ \bar{\mathbf{g}}_{\mathbf{2r_i}}\ \bar{\mathbf{g}}_{\mathbf{3r_i}} \right]_j \quad \text{for the } j\text{th pixel}$$

g_{0r} is roll-invariant (common to all transformation)

$\bar{\mathbf{g}}_{\mathbf{xr_i}}$ is a $N_s \times N_s$ vector; where the subscript $\mathbf{x}$ is either $\{1, 2, 3\}$

Data Set and Study Area

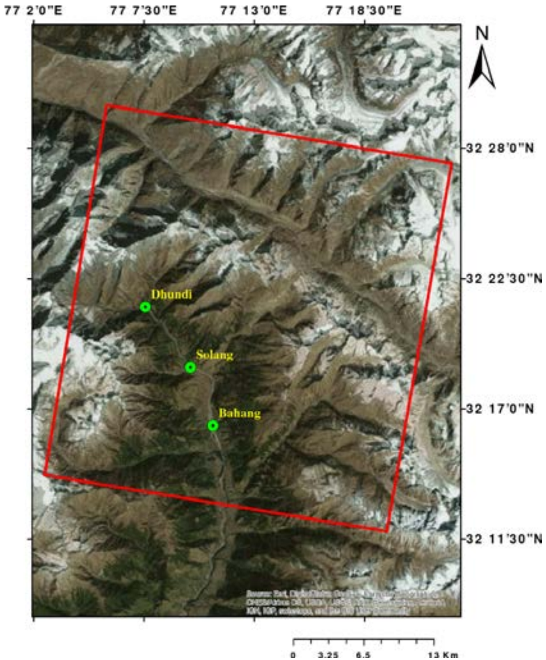

Meteorological observatories at Bahang (2000m), Solang (2450m) and Dhundi (2900m) are maintained in this area to record local climatic conditions.

- The test site is located in the **Manali-Dhundi** region of Himachal Pradesh, India
- The lower elevations of the area are covered with **coniferous forest**
- **SAR Data:**
- Radarsat-2
  - 18th March 2015 (Ascending 6:14am)
  - Resolution:
    - Azimuth: 5.1 m
    - Range: 11.8 m
  - Incidence angle: 46.0° – 47.2°

Optical Data:

- Landsat 8
  - 23rd March 2015
  - Resolution: 30m

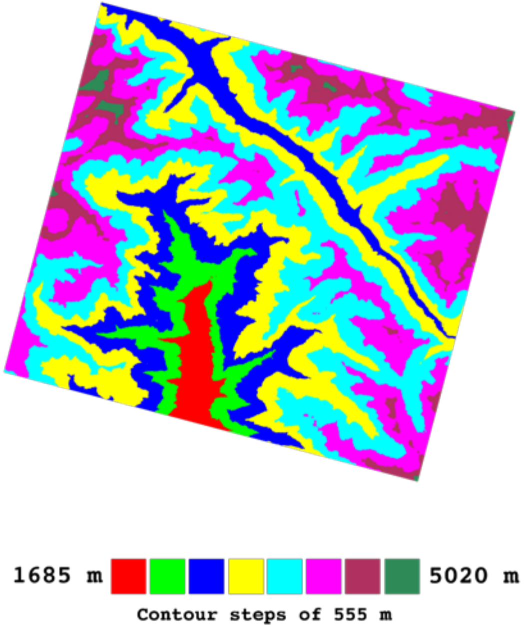

IIT Bombay

Results

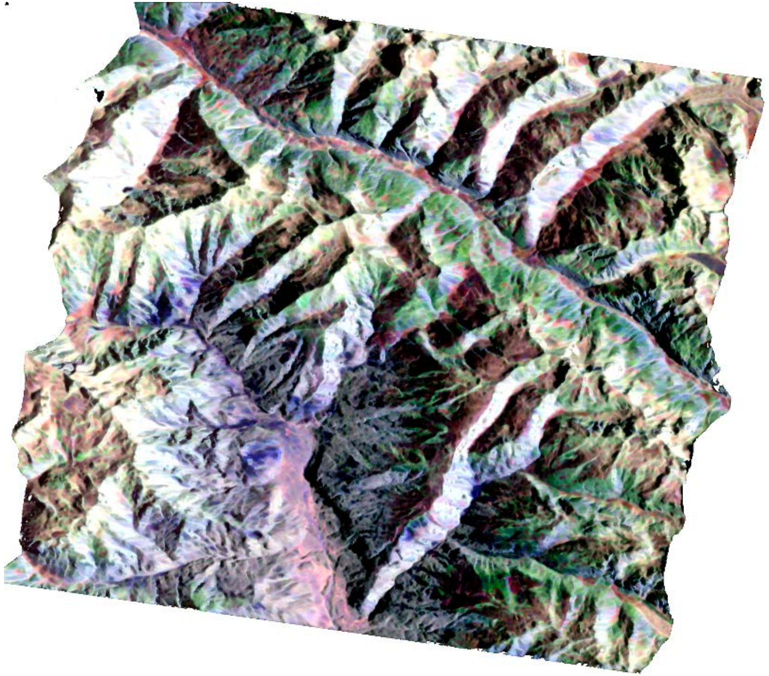

Radarsat 2

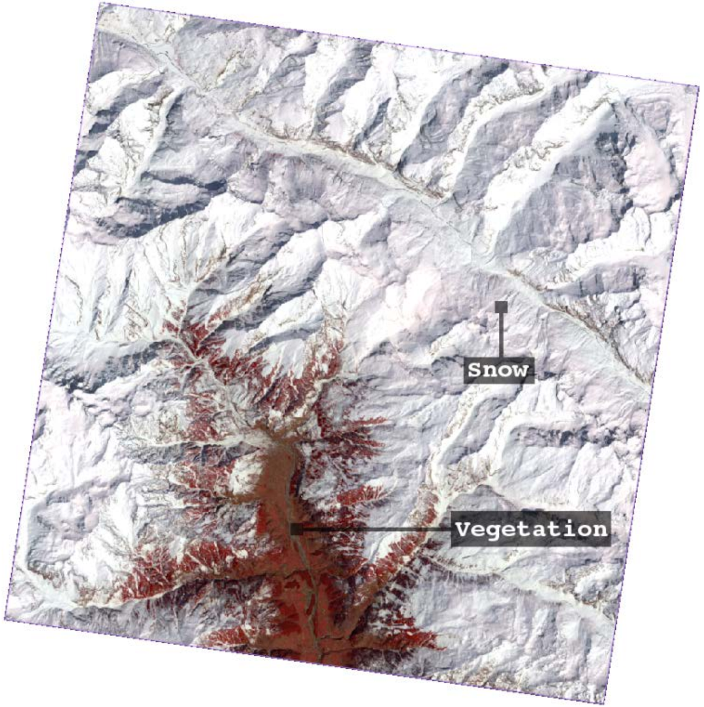

Landsat-8 FCC

Dominant Scattering Type Comparison

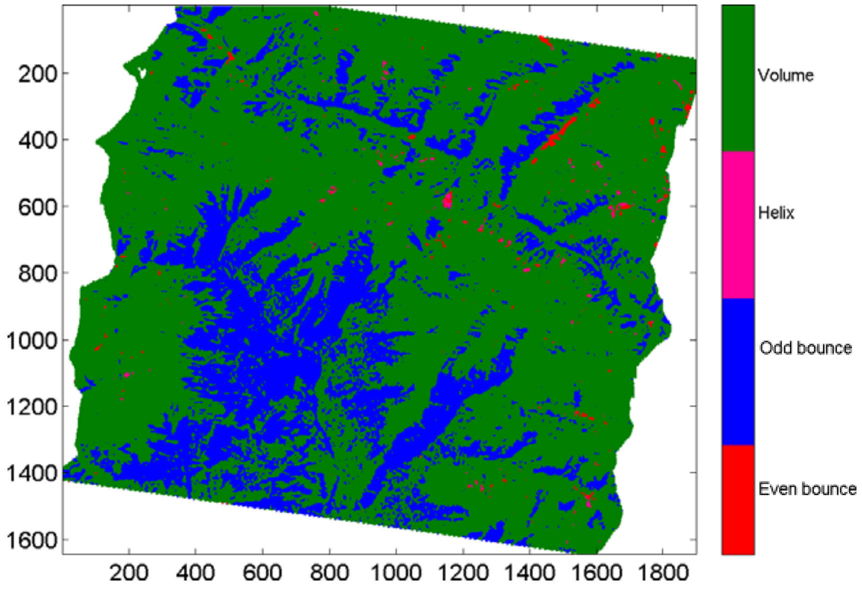

March 2015

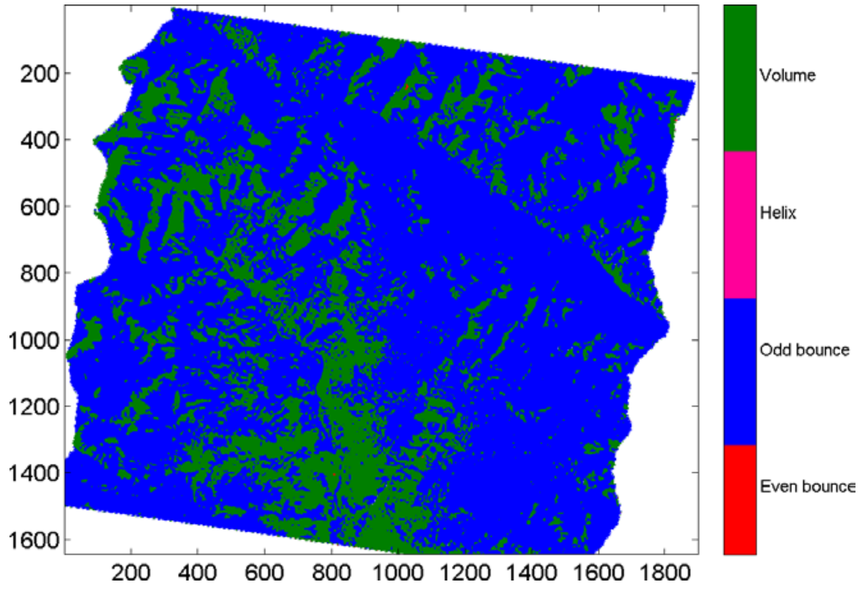

August 2015

Results

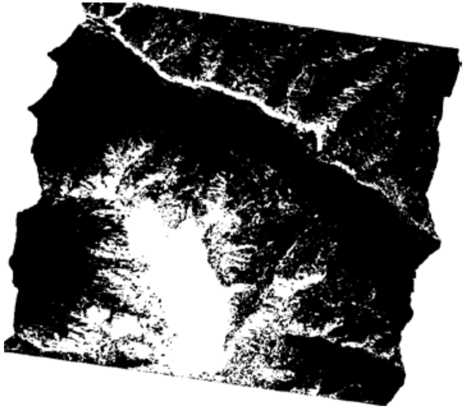

Reference Map

Snow   No-Snow

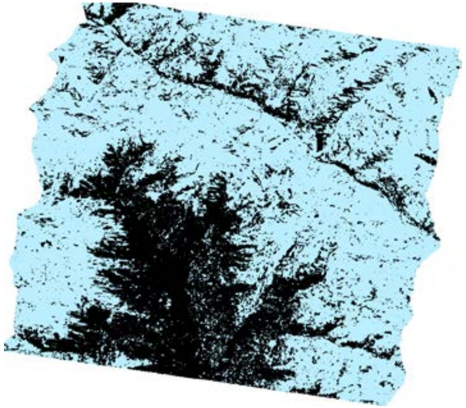

All $OA = 88.96\%, f_1 = 0.92$

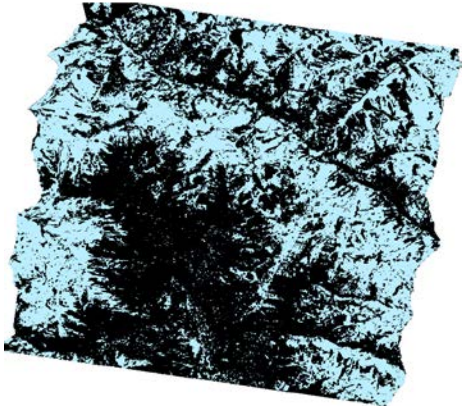

CIR $OA = 65.02\%, f_1 = 0.70$

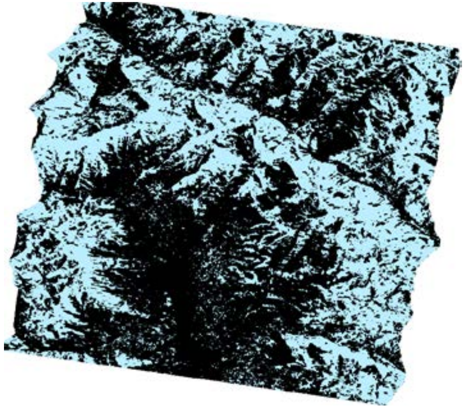

LIN $OA = 64.48\%, f_1 = 0.69$

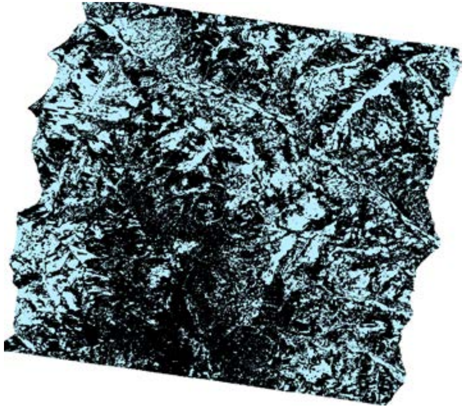

$\pi/4$ $OA = 52.89\%, f_1 = 0.58$

Results: Snow-Cover Percentage

Snow No-Snow

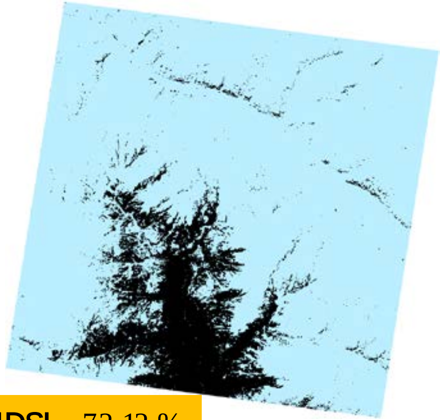

NDSI – 72.12 %

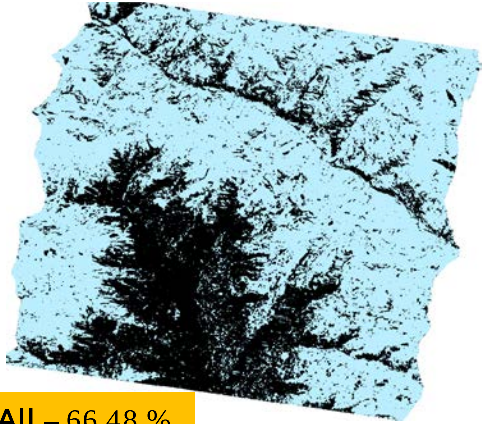

All – 66.48 %

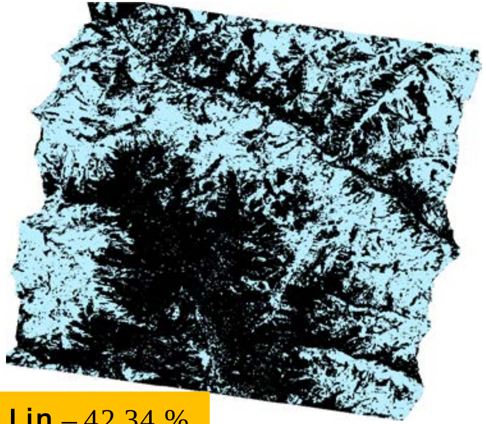

Lin – 42.34 %

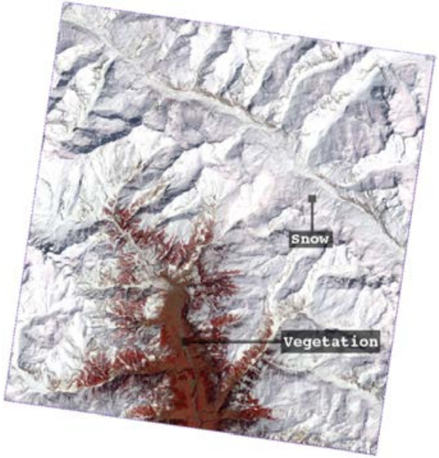

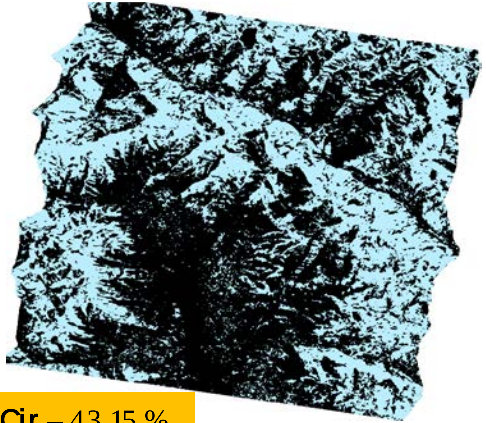

Cir – 43.15 %

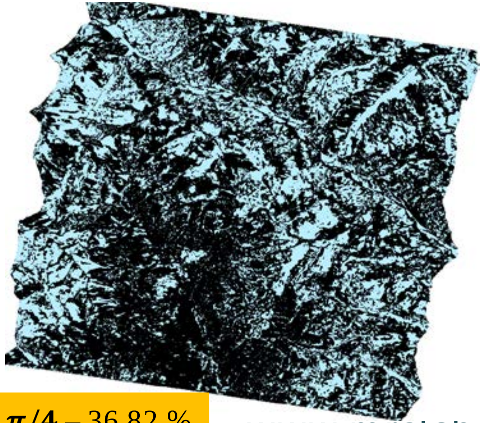

$\pi/4$ – 36.82 %

Classifier Comparison

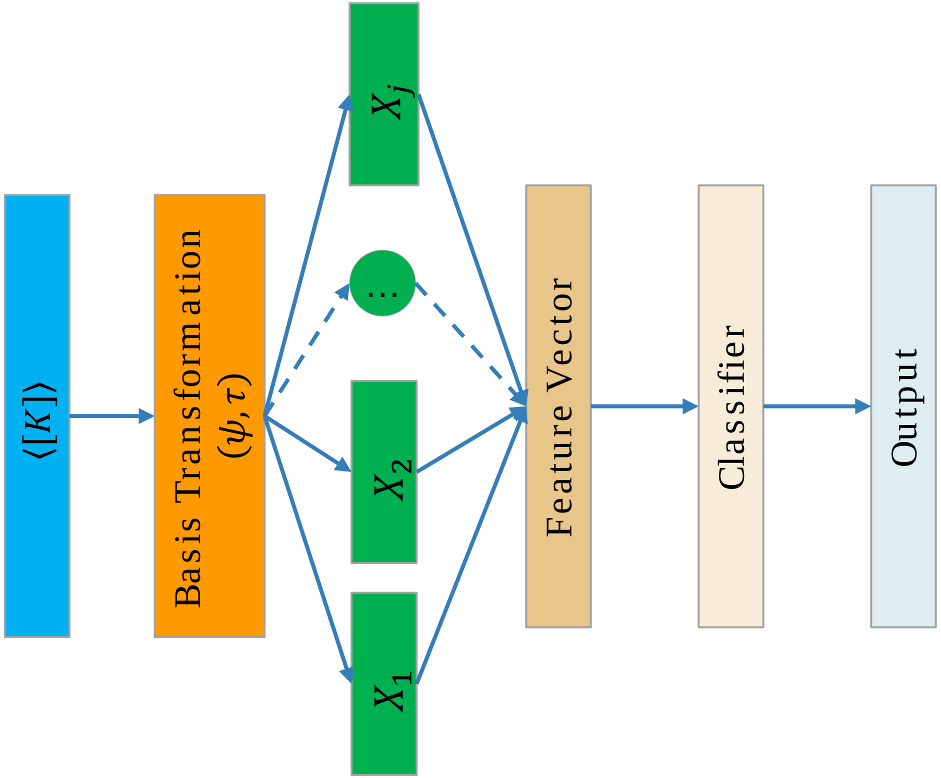

Classifier
AE + MLP
MLP
SVM (Lin)

Classifier Comparison

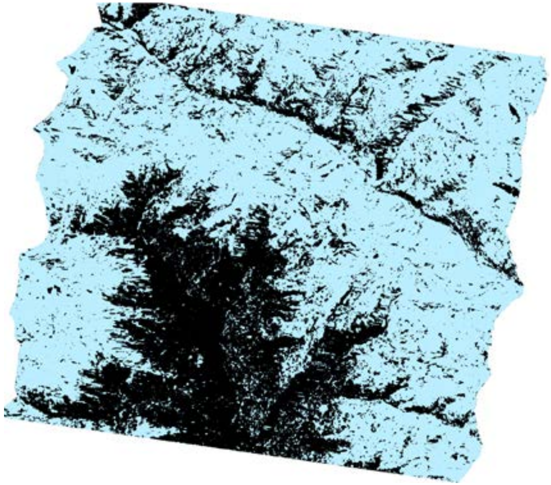
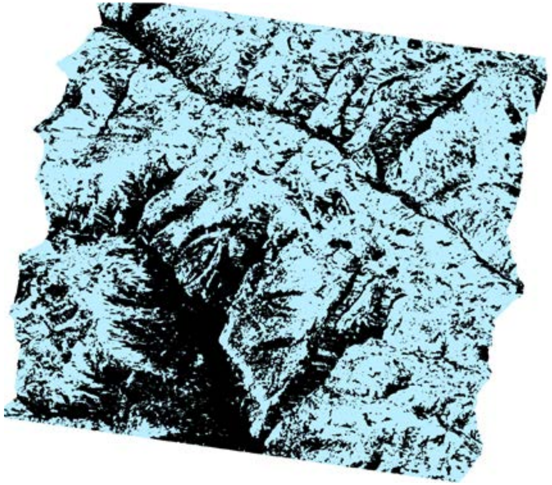
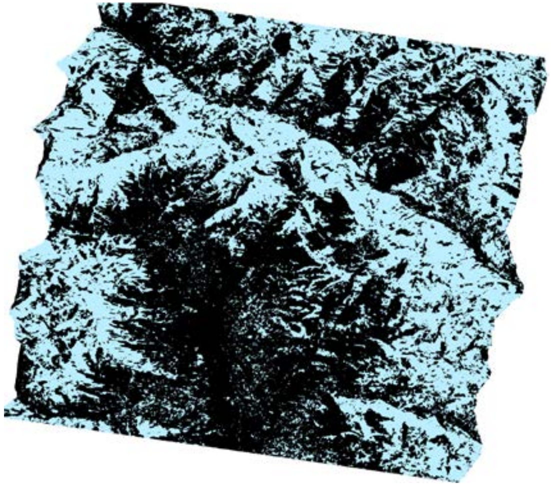

Proposed	MLP (no AE)	SVM (no AE, Lin)
OA = 88.96% $f_1 = 0.92$	OA = 75.39% $f_1 = 0.81$	OA = 65.56% $f_1 = 0.71$

Snow No-Snow

Overall Results

Numeric Accuracy Comparison			
Method	OA(%)	κ	f_1
ALL (proposed)	**88.96**	**0.73**	**0.92**
CIR	65.02	0.35	0.70
LIN	64.48	0.34	0.69
$\pi/4$	52.89	0.21	0.58
MLP ALL (no-AE)	75.39	0.45	0.81
SVM ALL (no-AE)	65.56	0.35	0.71

Snow-Cover Percent				
NDSI	ALL (proposed)	LIN	CIR	$\pi/4$
72.12	**66.48**	43.15	42.35	36.82

Summary & Future Scope

- The algorithms are unsupervised in nature.
- Thresholds are not locally determined &globally imposed.
- The investigation highlights the meteorological impacts on the polarimetric variables.
- The possible role of time of acquisition on the polarimetric analysis is highlighted.
- Algorithms are compatible with C-band PolSAR data.
- Introduction of Deep Learning techniques using PolSAR data

Thank You

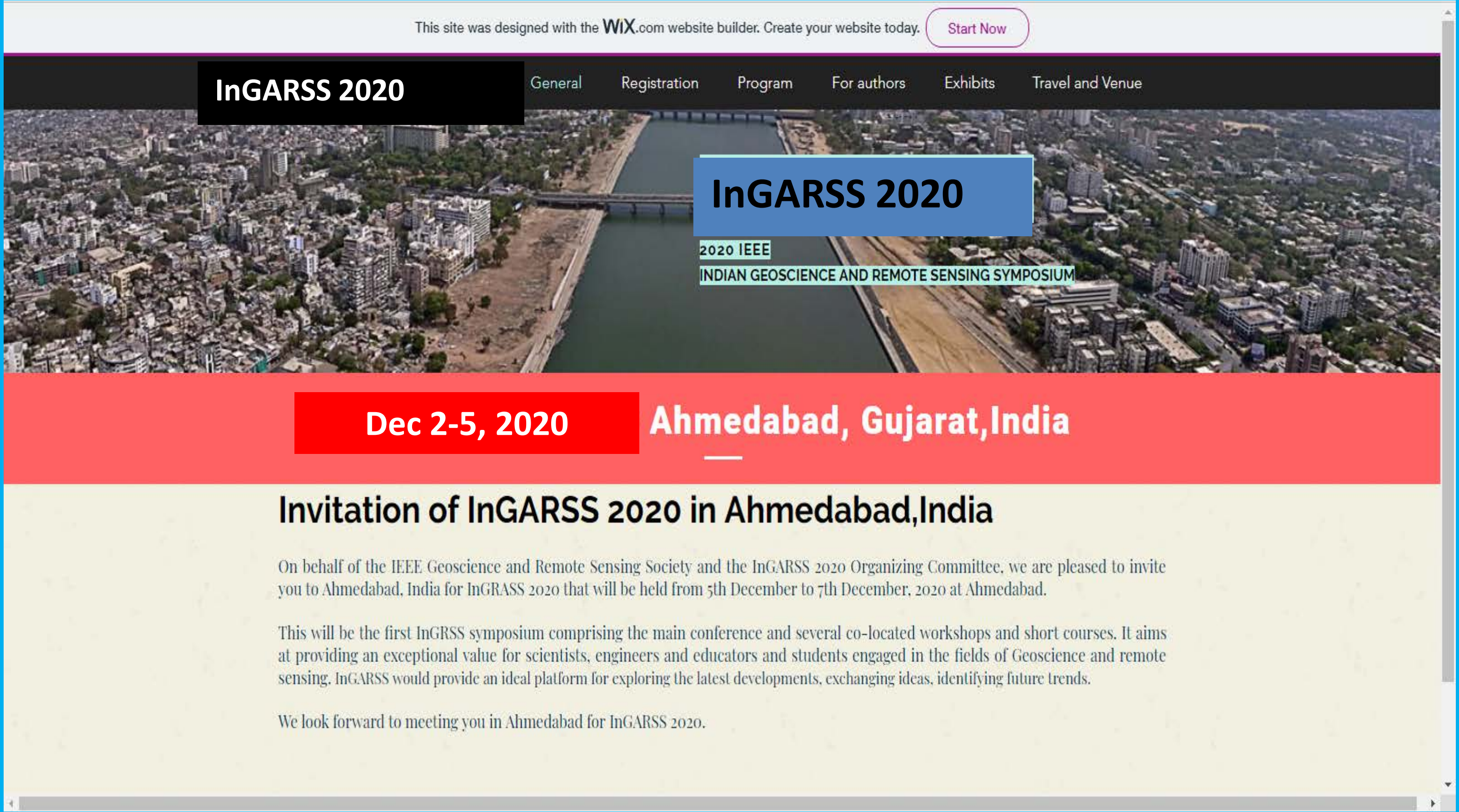

This site was designed with the WiX.com website builder. Create your website today. Start Now

InGARSS 2020

General | Registration | Program | For authors | Exhibits | Travel and Venue

InGARSS 2020

2020 IEEE

INDIAN GEOSCIENCE AND REMOTE SENSING SYMPOSIUM

Dec 2-5, 2020 **Ahmedabad, Gujarat, India**

Invitation of InGARSS 2020 in Ahmedabad,India

On behalf of the IEEE Geoscience and Remote Sensing Society and the InGARSS 2020 Organizing Committee, we are pleased to invite you to Ahmedabad, India for InGRASS 2020 that will be held from 5th December to 7th December, 2020 at Ahmedabad.

This will be the first InGRSS symposium comprising the main conference and several co-located workshops and short courses. It aims at providing an exceptional value for scientists, engineers and educators and students engaged in the fields of Geoscience and remote sensing. InGARSS would provide an ideal platform for exploring the latest developments, exchanging ideas, identifying future trends.

We look forward to meeting you in Ahmedabad for InGARSS 2020.